



# The Society for Immunotherapy of Cancer Perspective on Tissue-Based Technologies for Immuno-Oncology Biomarker Discovery and Application

Anne Monette<sup>1</sup>, Adriana Aguilar-Mahecha<sup>2</sup>, Emre Altinmakas<sup>3,4</sup>, Mathew G. Angelos<sup>5</sup>, Nima Assad<sup>6</sup>, Gerald Batist<sup>7</sup>, Praveen K. Bommareddy<sup>8</sup>, Diana L. Bonilla<sup>9</sup>, Christoph H. Borchers<sup>10,11</sup>, Sarah E. Church<sup>12</sup>, Gennaro Ciliberto<sup>13</sup>, Alexandria P. Cogdill<sup>14</sup>, Luigi Fattore<sup>15</sup>, Nir Hacohen<sup>16</sup>, Mohammad Haris<sup>17,18</sup>, Vincent Lacasse<sup>19</sup>, Wen-Rong Lie<sup>20</sup>, Arnav Mehta<sup>16</sup>, Marco Ruella<sup>21</sup>, Houssein Abdul Sater<sup>22</sup>, Alan Spatz<sup>23</sup>, Bachir Taouli<sup>3</sup>, Imad Tarhoni<sup>24</sup>, Edgar Gonzalez-Kozlova<sup>6</sup>, Itay Tiros<sup>25</sup>, Xiaodong Wang<sup>26</sup>, and Sacha Gnjatic<sup>6</sup>

## ABSTRACT

With immuno-oncology becoming the standard of care for a variety of cancers, identifying biomarkers that reliably classify patient response, resistance, or toxicity becomes the next critical barrier toward improving care. Multiparametric, multi-omics, and computational platforms generating an unprecedented depth of data are poised to usher in the discovery of increasingly robust biomarkers for enhanced patient selection and personalized treatment approaches. Deciding which developing technologies to implement in clinical settings ultimately, applied either alone or in combination, relies on weighing pros and cons, from minimizing patient sampling to maximizing data outputs, and assessing the reproducibility and representativeness of findings, while lessening data fragmentation toward harmonization. These factors are all assessed while taking into consideration the

shortest turnaround time. The Society for Immunotherapy of Cancer Biomarkers Committee convened to identify important advances in biomarker technologies and to address advances in biomarker discovery using multiplexed IHC and immunofluorescence, their coupling to single-cell transcriptomics, along with mass spectrometry-based quantitative and spatially resolved proteomics imaging technologies. We summarize key metrics obtained, ease of interpretation, limitations and dependencies, technical improvements, and outward comparisons of these technologies. By highlighting the most interesting recent data contributed by these technologies and by providing ways to improve their outputs, we hope to guide correlative research directions and assist in their evolution toward becoming clinically useful in immuno-oncology.

## Introduction

Immune checkpoint inhibitor (ICI) therapies have revolutionized cancer treatment. These successes are in part the result of biomarker developments that have enhanced our understanding of tumor-immune interactions and mechanisms of host immune evasion. In

2011, the first U.S. FDA-approved ICI was ipilimumab targeting cytotoxic T lymphocyte antigen 4 for advanced melanoma (1). Several other ICI agents have since been approved, including those blocking the PD-1/PD-L1 pathway for treating an ever-growing variety of cancers (2, 3). Whereas some patients achieve very

<sup>1</sup>Lady Davis Institute for Medical Research, Jewish General Hospital, Montreal, Quebec, Canada. <sup>2</sup>Lady Davis Institute for Medical Research, The Segal Cancer Center, Jewish General Hospital, Montreal, Quebec, Canada.

<sup>3</sup>Department of Diagnostic, Molecular and Interventional Radiology, Icahn School of Medicine at Mount Sinai, New York, New York. <sup>4</sup>Department of Radiology, Koç University School of Medicine, Istanbul, Turkey. <sup>5</sup>Division of Hematology and Oncology, Department of Medicine, University of Pennsylvania, Philadelphia, Pennsylvania. <sup>6</sup>Icahn School of Medicine at Mount Sinai, New York, New York. <sup>7</sup>McGill Centre for Translational Research, Jewish General Hospital, Montreal, Quebec, Canada. <sup>8</sup>Replimune Inc., Woburn, Massachusetts. <sup>9</sup>Cyttek Biosciences, Fremont, California. <sup>10</sup>Gerald Bronfman Department of Oncology, Segal Cancer Proteomics Centre, Lady Davis Institute for Medical Research, Jewish General Hospital, Montreal, Quebec, Canada. <sup>11</sup>Division of Experimental Medicine, Department of Pathology, McGill University, Montreal, Quebec, Canada. <sup>12</sup>Zymeworks Biopharmaceuticals Inc., Bellevue, Washington. <sup>13</sup>Scientific Direction, IRCCS Regina Elena National Cancer Institute, Rome, Italy. <sup>14</sup>Daiichi Sankyo, Inc., Basking Ridge, New Jersey. <sup>15</sup>SAFU Laboratory, Department of Research, Advanced Diagnostics and Technological Innovation, Translational Research Area, IRCCS Regina Elena National Cancer Institute, Rome, Italy. <sup>16</sup>Massachusetts General Hospital Cancer Center, Boston, Massachusetts. <sup>17</sup>Department of Radiology, Center for Advanced Metabolic Imaging in Precision

Medicine, Perelman School of Medicine, University of Pennsylvania, Philadelphia, Pennsylvania. <sup>18</sup>Laboratory Animal Research Center, Qatar University, Doha, Qatar. <sup>19</sup>Segal Cancer Proteomics Centre, Lady Davis Institute for Medical Research, Jewish General Hospital, McGill University, Montreal, Quebec, Canada. <sup>20</sup>MilliporeSigma, St. Louis, Missouri. <sup>21</sup>Division of Hematology-Oncology, Center for Cellular Immunotherapies, University of Pennsylvania, Philadelphia, Pennsylvania. <sup>22</sup>Cleveland Clinic, Carol and Robert Weissman Cancer Center, Stuart, Florida. <sup>23</sup>Lady Davis Institute for Medical Research, Jewish General Hospital, McGill University, McGill University Health Center, Montreal, Quebec, Canada. <sup>24</sup>Department of Anatomy and Cell Biology, Rush University Medical Center, Chicago, Illinois. <sup>25</sup>Department of Molecular Cell Biology, Weizmann Institute of Science, Rehovot, Israel. <sup>26</sup>Key Laboratory of Mass Spectrometry Imaging and Metabolomics, College of Life and Environmental Sciences, Minzu University of China, Beijing, China.

**Corresponding Author:** Anne Monette, Lady Davis Institute for Medical Research, Jewish General Hospital, 3755 Chemin de La Côte-Sainte-Catherine, Montreal H3T 1E2, Quebec, Canada. E-mail: anne.monette@mail.mcgill.ca

Clin Cancer Res 2024;XX:XX-XX

**doi:** 10.1158/1078-0432.CCR-24-2469

©2024 American Association for Cancer Research

positive outcomes from use of these immunomodulators, others do not respond or develop resistance or toxicities to ICI therapies (4).

Toward the eventual mainstay of ICIs as first-line therapy for any benefiting patient with cancer, robust biomarkers that can ultimately and unquestionably predict responses are critically needed and are thus currently being extensively studied and clinically validated in a subset of the 1,000 of ongoing ICI trials. From 1986 to 2025, the Cancer Research Institute database recorded more than 17,500 planned or ongoing global immuno-oncology (IO) clinical trials (5). Whereas the rate of indexed IO biomarker publications demonstrates a surge in predictive or prognostic reports over the last decade (**Fig. 1**), to date, the FDA has only approved three (3) tissue-based biomarkers for solid malignancies: IHC to detect PD-L1 upregulation on tumor cells (i.e., 22C3 PHARMDX, 28-8 PHARMDX, and SPI142 Ventana; refs. 6–8), tumor mutational burden (TMB) promoting T-cell infiltration (i.e., TMB-H FoundationOne CDx; refs. 9, 10), and microsatellite instability–high tumors from defective DNA mismatch repair (refs. 11, 12). The challenges that have been met using these predictive biomarkers have highlighted critical areas to improve in the discovery, development, and standards of reporting for future companion diagnostics (CDx; refs. 13–18). Just as different groups came together to compare different PD-L1 antibodies at the time when they started gaining approval (19, 20), so have others like the Friends of Cancer Research TMB Harmonization Consortium to characterize empirical variability of mutation assessment across platforms (16, 18). Harmonization and standardization collectives and efforts will become even more critical as these high-dimensional technologies continue to advance, and the sharing of data between groups to compare cross-platform and laboratory reproducibility and variability will be a prerequisite for any new approvals [for reviews on conceptual and practical challenges of data sharing for biomarker development, please see (21, 22)]. As IO response biomarker discovery practices move ahead, so does the growing list of other types of CDx biomarker classifiers to include for monitoring or measuring toxicity (**Fig. 1**).

Many new areas of biomarker development in testing include those investigating the tumor microenvironment (TME) using multiplex IHC (mIHC), immunofluorescence (IF), gene expression profiling, microbiome investigations, and those examining soluble biomarkers from liquid biopsy. With the many different biomarker types under investigation has come the development of various new technologies that may, used either alone or in combination, provide the most robust biomarkers for ICIs and other therapeutic IO approaches. This article addresses leading novel IO biomarker technologies and describes key advances made to earlier approaches. The main technologies covered in this report are advances in multiplex tissue staining, including proteomic profiling and transcriptomics techniques. Subsections provide a historic overview highlighting principles and details of techniques where necessary, their key metrics and measurement obtained, and their ease of interpretation, limitations and recent technical improvements, and dependencies or adaptabilities for coupling to other technologies, in addition to comparisons made to other similar technologies. Finally, we discuss interesting data contributed by these technologies, highlight ongoing or completed trials utilizing them, and demonstrate how some provide seminal IO biomarker discoveries that may soon influence routine therapeutic regimens.

## **Tissue Multiplexing with Single-Cell Sequencing Provides Ultimate Spatial Resolution**

Tissue architecture and spatial distribution of cellular components are vital to maintaining tissue homeostasis and numerous

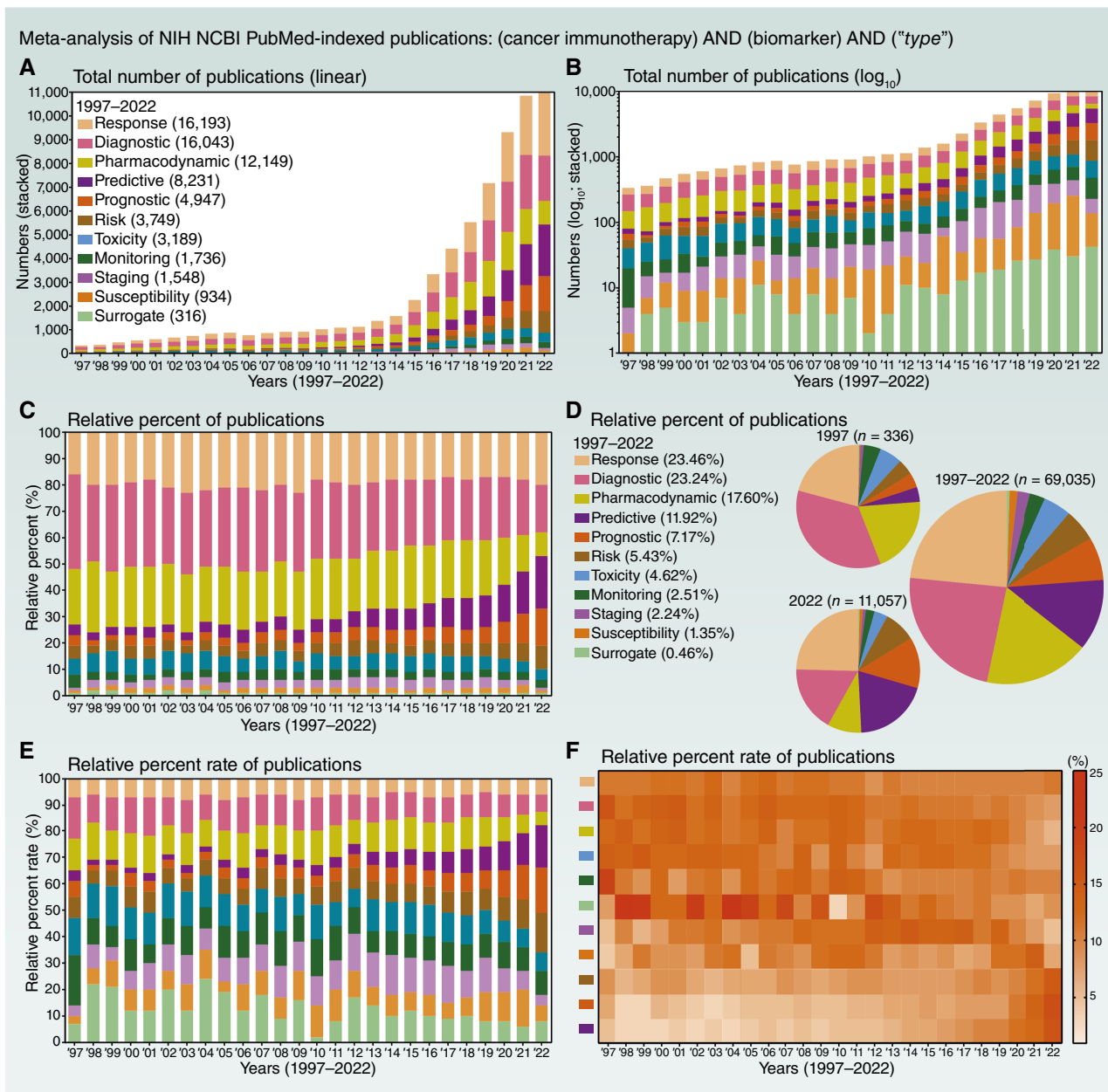
natural cellular processes. Characterization of cellular dynamics during conditions of physiologic stress, such as infection, autoimmune disorders, and cancer, is important for establishing diagnosis and identifying targets for novel therapeutics. Therefore, mapping cellular topography and interactions within tissue is critical for understanding the key drivers of immune function (23). Tissue-based imaging technologies provide important spatial information for biomarker pursuits. Spatial, from Latin “spatium” for space, describes the perception of relationships between objects relative to their proximity. The application of spatial concepts to biology has led to a systems biology framework, in which each interactive element is considered to be influenced by all others within its environment, and thus the characterization of all components of biological systems on a much more comprehensive scale.

The characteristic molecular properties of each individual cell are best understood by the mapping of its physical location, in which its specific gene expression program is both influencing and being influenced by the rest of the cells within its distinct tissue microenvironment. Systems immunology is the new frontier for the phenotyping of autonomous immune cells that can be found in all tissues and are mobilized in response to gradients of cues (24). Despite numerous initiatives in classifying the TME (refs. 25–28), it is especially challenging as a result of the undermining of cancer cell subpopulations that provide unique structures and gene expression profiles influencing immunity and intratumor heterogeneity (29). It has been suggested that progress using tumor bulk may only be possible on a per-patient or -tumor basis using computational oncology (30).

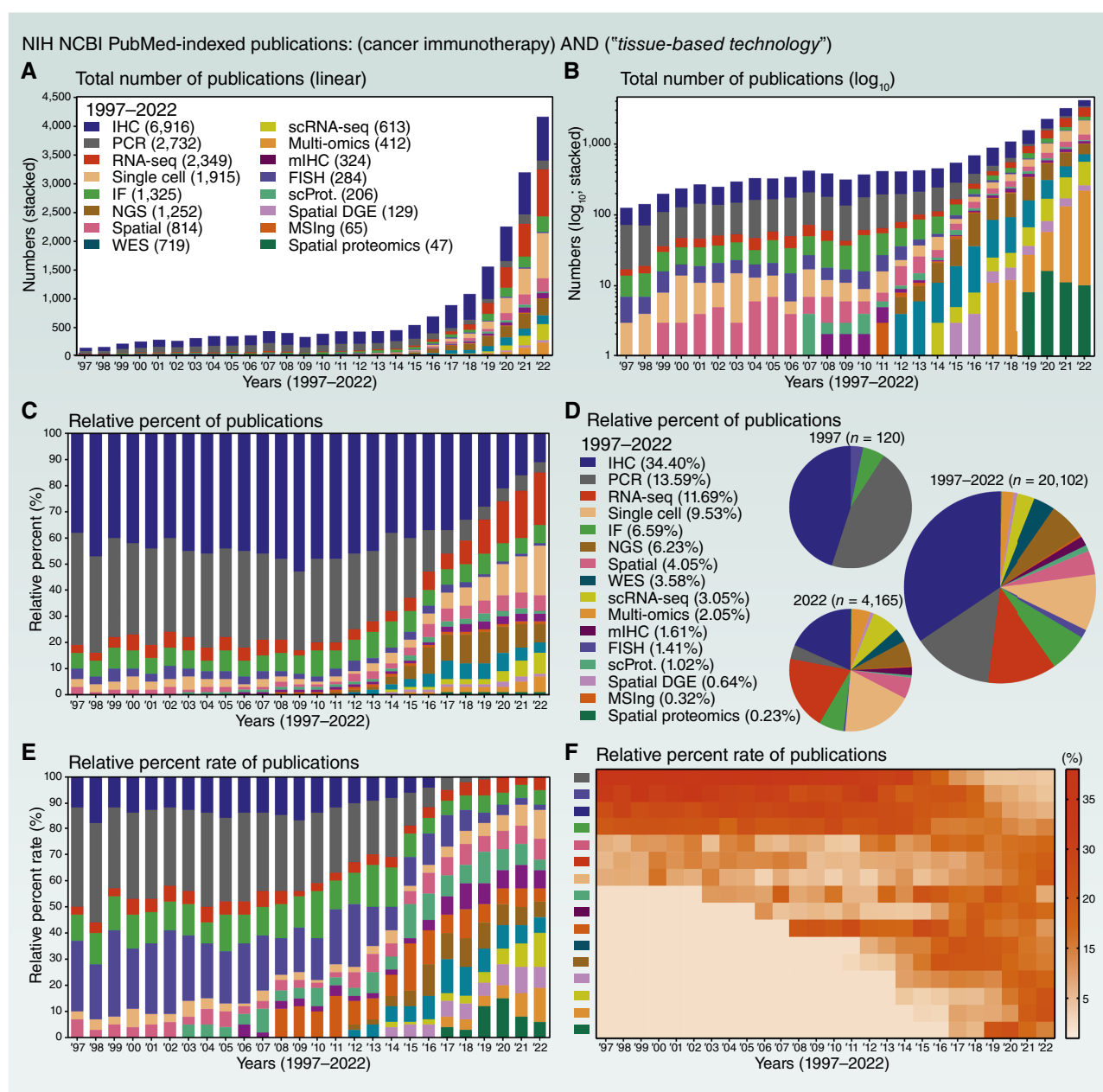
Experimental platforms such as single-cell transcriptomics have enabled high-dimensional gene profiling of immune cells (31) and high-resolution characterization of a much greater number of immune cell subsets than previously appreciated (32). However, tissue digestion and processing obfuscates spatial organization and compromises the study of cell-cell interaction and higher-order tissue structures influencing or impeding immunity (33, 34). Tissue imaging platforms such as IHC, although retaining tissue organization, are limited to visualizing predefined sets of protein markers and are limited in the number of proteins that can simultaneously be visualized. Thus, characterizing spatial distributions of immune cells and their cellular partners in tissues has remained challenging.

Most often, traditional microscopy techniques are those used to characterize cellular composition and tissue architecture. These microscopy techniques often include IHC, IF, and other low-throughput approaches limiting the detection to only a couple of cell types in the TME. This narrow capture limits the opportunity to gain insights into the diagnosis and prognostication of the disease relative to the broader landscape of cellular architecture offered in the holistic images derived from multiplex approaches. The last decade witnessed the rapid development of several mIHC/IF approaches to overcome the limitations of conventional single-marker techniques. These technologies permitting simultaneous detection of multiple markers on a single slide of tissue are poised for adoption by preclinical and clinical research (35). Several multiplexed IHC/IF techniques have emerged to permit comprehensive studies of TME composition, cell-to-cell spatial interactions, and differentiation and activation status of immune cells (**Fig. 2**; ref. 36).

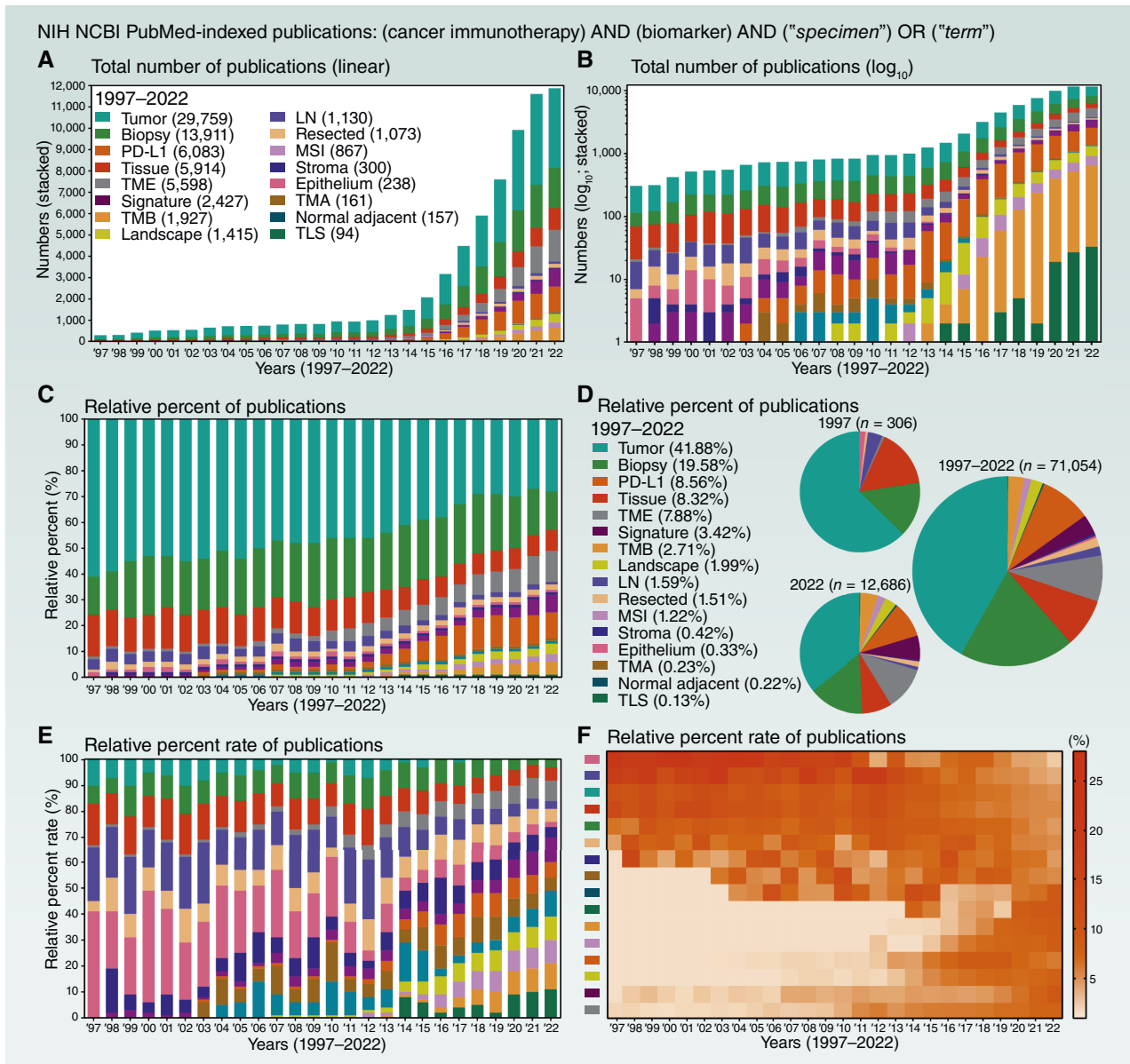
Whereas mIHC/IF can provide spatial information on the protein produced by cells within the TME (36), even the best current technologies can still only plex up to ~40 targets (37). Spatial transcriptomics that can deliver a snapshot deciphering gene expression levels and positional arguments for up to 5,000 RNAs per cell may indeed provide the

**Figure 1.**

Chronologic meta-analysis of NCBI-indexed publications of different types of biomarkers. Publications indexed on NIH NCBI PubMed (<https://pubmed.ncbi.nlm.nih.gov/>) were filtered according to search terms (cancer immunotherapy) AND (biomarker) AND biomarker types, including (prognostic), (predictive), (response), (diagnostic), (staging), (monitoring), (pharmacodynamic), (surrogate), (susceptibility), (toxicity), or (risk). Years spanning 1997–2022 were selected due to first FDA approvals of immunotherapies rituximab and IL-2 in 1997 and 1998, respectively. The results from years 1997 to 2022 were downloaded as .CSV files, and data were imported into Microsoft Excel software and converted to .XLSX files for organizing, harmonizing, and calculating the numbers, percentages, and rates of publication prior to import into GraphPad Prism v8.0.1 software for data visualizations that were exported as .PDF files later merged as figure panels using Adobe Illustrator CC software, demonstrating (A and B) the absolute number of indexed publications per year illustrated by (A) linear and (B)  $\log_{10}$  transformed stacked bar graphs, (C and D) the relative percent of indexed publications per year illustrated by (C) stacked bar graphs and (D) parts of whole pie charts of all or selected years, and (E and F) the relative percent rates of indexed publications per year illustrated by (E) stacked bar graphs and (F) heat maps. All graphical illustration colors identical to those found in legends presented in A and D.

**Figure 2.**

Chronologic meta-analysis of NCBI-indexed publications of current and emerging IO biomarker discovery tissue-based technologies. Publications indexed on NIH NCBI PubMed (<https://pubmed.ncbi.nlm.nih.gov/>) were filtered according to search terms (cancer immunotherapy) AND different tissue-based technologies, including (IHC), (mlHC), (IF), (FISH), (single-cell), (RNA-seq), (scRNA-seq), (single-cell proteomics), (spatial), (spatial differential gene expression), (spatial proteomics), (PCR), (whole exome sequencing), (next-generation sequencing), (MSIng), or (multi-omics). Years spanning 1997–2022 were selected due to first FDA approvals of immunotherapies rituximab and IL-2 in 1997 and 1998, respectively. IHC was included to permit contrast relative to LBx and radiomics results. The results from years 1997 to 2022 were downloaded as .CSV files, and data were imported into Microsoft Excel software and converted to .XLSX files for organizing, harmonizing, and calculating the numbers, percentages, and rates of publication prior to import into GraphPad Prism v8.0.1 software for data visualizations that were exported as .PDF files later merged as figure panels using Adobe Illustrator CC software, demonstrating (A and B) the absolute number of indexed publications per year illustrated by (A) linear and (B)  $\log_{10}$  transformed stacked bar graphs, (C and D) the relative percent of indexed publications per year illustrated by (C) stacked bar graphs and (D) parts of whole pie charts of all or selected years, and (E and F) the relative percent rates of indexed publications per year illustrated by (E) stacked bar graphs and (F) heat maps. All graphical illustration colors identical to those found in legends presented in A and D. DGE, differential gene expression; NGS, next-generation sequencing; scProt, single-cell proteomics; WES, whole exome sequencing.

**Figure 3.**

Chronologic meta-analysis of NCBI-indexed publications of biospecimen types and terms used for IO biomarker discovery. Publications indexed at NIH NCBI PubMed (<https://pubmed.ncbi.nlm.nih.gov/>) were filtered according to search terms (cancer immunotherapy) AND (biomarker) AND (tumor), (tissue), (biopsy), (lymph node), (stroma), (epithelium), (resected), (tissue microarray), (normal adjacent), (TME), (tertiary lymphoid structures), (signature), (landscape), (PD-L1), (TMB), or (microsatellite instability). Years spanning 1997–2022 were selected due to the first FDA approvals of immunotherapies rituximab and IL-2 in 1997 and 1998, respectively. The results from years 1997 to 2022 were downloaded as .CSV files, and data were imported into Microsoft Excel software and converted to .XLSX files for organizing, harmonizing, and calculating the numbers, percentages, and rates of publication prior to import into GraphPad Prism v8.0.1 software for data visualizations that were exported as .PDF files later merged as figure panels using Adobe Illustrator CC software, demonstrating (A and B) the absolute number of indexed publications per year illustrated by (C) linear and (B)  $\log_{10}$  transformed stacked bar graphs, (C and D) the relative percent of indexed publications per year illustrated by (C) stacked bar graphs and (D) parts of whole pie charts of all or selected years, and (E and F) the relative percent rates of indexed publications per year illustrated by (E) stacked bar graphs and (F) heat maps. All graphical illustration colors identical to those found in legends presented in A and D. LN, lymph node; MSI, microsatellite instability; TLS, tertiary lymphoid structure; TMA, tumor microarray.

comprehensive information required to gain important information about the actual biological meaning (38), with the drawback of reading RNAs rather than actual proteins produced by cells of interest. In this study, we review the landscape of several staple and more recent tissue-based spatial techniques and biospecimen features and types that are revolutionizing our understanding of the TME and have the power to resolve biomarker research for IO (Fig. 3).

### Advances in mIHC and IF for TME characterization

Despite the wide popularity of IHC and IF as conventional research and diagnostics methods, an appreciation of the fundamentals and the evolutions of these methods may lay the groundwork for advancing these technologies to accommodate the demand for high-throughput data. Biomarker discovery in tissues began with a red protein dye (i.e., R-salt-azo-benzidine-azo-crystalline egg albumen; ref. 39) conjugated to benzidin tetraedro against typhus and cholera microorganisms by Marrack and colleagues (40) and fluorescein-stained antibodies against *Streptococcus pneumonia* for visualization by UV light by Coons and colleagues (41). Marked antibodies made visible for optical and fluorescent microscopy by Nakane and colleagues (42) brought this technology to many more researchers and pathologists. Peroxidase-antiperoxidase by Sternberger and colleagues (43) and alkaline phosphatase-antialkaline phosphatase by Mason and colleagues (44) significantly expanded IHC applications. Diaminobenzidine molecule conjugation to antibodies by Singer and colleagues (45) and the use of gold colloidal particles for coloration by Faulk and colleagues (46) led to subcellular resolution. Antigen retrieval by Huang and colleagues (47) and secondary antibody detection by Hsu and colleagues (48) led to IHC in fresh and fixed tissues. Pursuant detection of tissue antigens by immunoperoxidase in formalin-fixed paraffin-embedded (FFPE) tissues led to the “brown revolution” of IHC adoption in routine diagnostic pathology (49–52), with an exponential increase of ~100,000 publications on IHC in the following two decades (53).

The advent of mIHC/IF technologies permitting the simultaneous detection of many markers on a single tissue section have been adopted in research and clinical settings in response to increased demand for improved diagnostic techniques permitting comprehensive studies of functional cellular states and spatial information for cell-to-cell interaction within complex TMEs (54). Antibody-based staining for multiple target antigens within a single tissue section has offered unique opportunities to sparingly study complex TMEs in scarce patient samples. Antibody conjugates used to detect signals are either chromogenic (IHC, e.g., Cell ID<sup>x</sup>/Ultraplex, DISCOVERY ULTRA system), immunofluorescent (IF, e.g., Opal, MultiOmyx), or DNA barcode-based [PhenoCycler-Fusion (formerly codetection by indexing; CODEX), NanoString; ref. 36]. The major limitations of these technologies lie in pre-analytic challenges of staining FFPE tissues, analytic complexity pertaining to signal detection, scanning abilities, and tumor heterogeneity, the need to build tissue microarrays to decrease cost, and postanalytic data queries. The IO revolution saw multiplexing technology manufacturers collaborate to develop better products supporting TME research. These products include Opal and PhenoCycler-Fusion (Akoya Biosciences), Cell DIVE (formerly MultiOmyx; NeoGenomics Laboratories), Cell ID<sup>x</sup>/UltraPlex (Leica Biosystems), InSituPlex (Ultivue), GeoMx Digital Spatial Profiler (NanoString), cytometry by time of flight (CyTOF; Fluidigm),

multiplexed ion beam imaging (MIBI) technology (Ionpath), DISCOVERY ULTRA (Roche), and ChipCytometry (Zellkraftwerk).

Whereas most multiplex IHC/IF studies have been discovery-oriented, more recent efforts have focused on validating their clinical utility (55). The use of 5-μm-thick FFPE tissue sections and automated staining (Leica Bond, Discovery Ultra) is a routine practice in pathology laboratories. Standards in staining protocols and validation methodology are becoming better developed and defined by the multiplexing community (56, 57), and meta-analyses have demonstrated the potential superiority of multiplexing over other biomarker modalities for predicting response to PD-1/PD-L1 checkpoint blockade (54). Despite theoretical discrepancy between pathologist scoring and automated segmentation methods used in multiplexing image analysis, recent data suggests these are rather in high concordance (55). In order to support clinical adoption of multiplexing, Akoya Biosciences and other companies have launched several clinical research efforts and now operate a clinical-stage laboratory with Clinical Laboratory Improvement Amendments (CLIA) certification. Despite their growing popularity and promise, the significant spectral overlaps in fluorescence or visible colors from multiplex approaches can make it cumbersome to robustly analyze more than five to six fluorophores with precise identification and confidence (58). Therefore, limiting the number of markers observed in any specific multiplex panel makes this technology easier to accept by pathology communities.

mIHC/IF allows more accurate cellular phenotyping (59) and better assessment of spatial relationships among cells and compartments within the TME (60), which may predict clinical outcomes (61). The opportunity that will unveil itself is finding common spatial metrics of clinical utility. Artificial intelligence and astronomy-influenced image analyses provide powerful tools to advance this field. In a seminal paper by Berry and colleagues (62), the use of whole-slide AI-based “AstroPath” platform has identified key features in pretreatment melanoma specimens that predicted response to anti-PD-1-based therapy. The main factor limiting widespread adoption of this and other technologies is the number of specimens available for analyses. Multiplexing technologies have seen many advances over the last two decades and should be poised to assist in clinical trials designed to incorporate predictive biomarkers. For example, the ADaptiVe biomarker trial that InformS Evolution of therapy (ADVISE; NCT03335540) is a study with real-time biomarker-guided IO agent selection on limited pretreatment biopsies. In this study, we focus on mIHC/IF and its path(s) to becoming routinely used by the clinic. Whereas important advances in other multiplexing technologies are also addressed, it is judicious to consider that greater efforts will be required to establish any mIHC/IF panel as CDx, and the ultimate reproducibility of data by this technology remains the most rigorous way of assessing its clinical validity.

### PhenoCycler-Fusion: single-cell phenotypes and spatial relationships via DNA-conjugated antibodies

Even with the recent advent of existing multiplexed approaches, significant overlap in excitation and emission spectra still make it cumbersome to analyze more than five to six fluorophores with precise identification and low spectral overlap (58). Flow-based cytometry techniques widely gaining clinical acceptance are simultaneously immunophenotyping numerous cell types. However, disruption of the TME architecture during tissue dissociation for single-cell suspensions required for these techniques still represents a critical limitation. To overcome these limitations associated with

low-throughput microscopy and IHC techniques and to capture the full spectrum of cellular distribution, cell-cell interactions, and tissues architecture from a single section of tissue, the Nolan laboratory developed a highly multiplexed cytometric imaging approach, termed CODEX (ref. 63). This high-throughput technique, commercialized by Akoya Biosciences as “PhenoCycler-Fusion,” relies on DNA-conjugated antibodies and the cyclic addition and removal of complementary fluorescently labeled DNA probes for simultaneous visualization of up to 60 markers *in situ*. PhenoCycler-Fusion enables a deep view of single-cell spatial relationships within tissues toward accelerated discoveries across diseases. PhenoCycler-Fusion can provide precise information on cancer and immune cell distributions, their subtypes, and their activation status within the TME. The key component of the PhenoCycler-Fusion (CODEX) technology is partial reduction of IgG antibody disulfide bonds in the IgG antibody with tris [2-carboxyethyl] phosphine to conjugate it to a unique maleimide-modified DNA oligonucleotide or “barcode” (64). To create PhenoCycler-Fusion antibody panels, these unique DNA oligonucleotides can be conjugated for up to 57 reporter antibody targets of interest. Implementation of PhenoCycler-Fusion involves staining a tissue section with a unique DNA-conjugated antibody, adding the corresponding fluorescent oligonucleotide, and hybridizing this fluorophore with the conjugated antibody for visualization ahead of the chemical stripping of the fluorescently tagged oligonucleotide from the tissue and iteratively repeating this process for all targets of interest.

Recent advances in IO have triggered high interest to understand the spatial distribution of various immune cell subtypes and their functional status within the TME. The original 56 target PhenoCycler-Fusion (CODEX) panel was comprised of immune, tumor, and structural markers as well as immunomodulatory molecules to simultaneously phenotype, localize, and quantify these functional molecules on individual cells within the TME (65). This panel has since become adaptable and modifiable to include additional targets of interest. An ultrahigh-plex 101 target PhenoCycler-Fusion panel composed of markers of the key hallmarks of cancer was developed for a more broad-ranging interrogation of head and neck squamous cell carcinomas TMEs (66). Aside from this, a meta-analysis has validated that mIHC/IF has diagnostic accuracy comparable with other approaches for predicting response to anti-PD-1/PD-L1 (54). In that study, tumor specimens representing 8,135 patients having 10 different solid tumor types were assayed, and the results were correlated with anti-PD-1/PD-L1 response. Each modality was then evaluated with summary receiver operating characteristic (sROC) curves, providing comparable AUCs for ICI responses. However, mIHC/IF was shown to provide a significantly higher AUC (0.79) relative to PD-L1 IHC (AUC, 0.65;  $P < 0.001$ ), GEP (gene expression profiling; AUC, 0.65;  $P = 0.003$ ), and TMB (AUC, 0.69;  $P = 0.049$ ) alone. Additional studies with mIHC/IF and composite approaches with a larger number of patients will be required to further validate these findings. More recently, PhenoCycler-Fusion multiplexed tissue imaging on a tissue microarray derived from patients with advanced cutaneous T-cell lymphomas in a pembrolizumab trial (NCT02243579; ref. 67) identified topographic differences between immune cells, leading to development of the SpatialScore biomarker correlating with ICI responses and coinciding with differences in the tumor cell-specific chemokine recruitment and functional immune state of the TME, as validated using the commercial Vectra system (68). PhenoCycler-Fusion was also used in other trials (e.g., NCT04249739) in which it could demonstrate differential TME remodeling in responding

versus nonresponders by comparing pre- and post-treatment advanced gastric cancer biopsies (69).

The PhenoCycler-Fusion technology shares several limitations with more traditional mIHC/IF approaches, including high FFPE antibody costs and the requirement of repeatedly stripping tissues, which can impair downstream reiterative target antibody binding. Maleimide-modified DNA oligonucleotides are also expensive, as are fluorescently tagged DNA oligonucleotides (64). Additional manpower and work hours are required for conjugation of individual antibody and unified staining validation. The lack of availability of certain antibodies may pose issues, and the lack of signal amplification for low abundance proteins represents additional limiting factors. As for other multiplexing technologies that sample an ever-increasing number of antigens, region sizes and sample sizes providing large-scale and high-dimensional imaging data and advanced algorithms are required to delineate the cell clustering and image analysis. PhenoCycler-Fusion (CODEX) developers have been creating faster and more accurate processing to ensure reliable segmentation and identification of cell types, as well as to characterize neighborhoods and infer mechanistic insights. RAPID, a real-time, graphics processing unit (GPU)-accelerated parallelized image processing software for large-scale multiplexed fluorescence microscopy data, has been developed to deconvolve, stitch, and register images with axial and lateral drift correction and to minimize autofluorescence (70). Indeed, a geometric deep learning tool for cell-type discovery and identification in spatially resolved single-cell datasets called STELLAR was coupled with PhenoCycler-Fusion (CODEX) to more easily assign cells to cell types present in the annotated reference datasets and discover novel cell types and cell states (71).

Whereas this represents a very important discovery technology, to date, PhenoCycler-Fusion-based experiments have mainly used antibody-based detection of proteins of interest. Future development of this technology may include the labeling of nucleic acids to enable the codetection of nucleic acids that can open the possibility of investigating causative mutations or posttranscriptional modifications. Like many of the other technologies we discuss, with growing panel sizes, PhenoCycler-Fusion may be poised to characterize disease progression and the evolution of the TME during applied immunotherapy regimens.

### Single-cell RNA sequencing: TME gene expression and T-cell receptor sequencing

Single-cell RNA sequencing (scRNA-seq) has emerged as a powerful tool to characterize tumor cell heterogeneity (72, 73). Unlike many other single-cell methods, scRNA-seq provides an unbiased view of the expression of all genes, thereby making it a systematic approach to describe the cellular composition of any sample, while enabling unexpected discoveries that targeted or bulk approaches might miss. In addition to its direct output, gene expression by scRNA-seq can also be used to infer additional cellular features, and, most notably in the context of IO research, T-cell receptor sequences (74, 75). Other potential features include inferring splice variants, chromosomal copy-number aberrations (76), and possibly even future cellular states (77), although such methods will require expertise and careful interpretation.

Still a relatively new technique for the number of applications it has now been used for, scRNA-seq was developed in 2011 by Tang and colleagues (78) and multiplexed by Islam and colleagues (79). ScRNA-seq libraries were developed (80), and soon after,

commercial cell isolation and library generation were made into a two-step process using microfluidics, greatly reducing the required time and labor (81, 82). scRNA-seq platforms have been continuously optimized (83) until the advent of the first portable plug-and-play single-cell library preparation procedure called Seq-Well (84).

ScRNA-seq has led to an improved understanding of tumor cell evolution during immunotherapy, the identification of malignant subclones, and the characterization of cellular components composing the TME (85). Clinically significant advancements through novel biomarker identification via scRNA-seq have been achieved for both hematologic malignancies (86–89) and solid tumors (90–93) over the last several years (others in addition to scRNA-seq–determined TME targets reviewed in ref. 94). A prominent example is its use in predicting clinical response to anti-CD19 chimeric antigen receptor T-cell (CAR T-cell) therapy in patients with diffuse large B-cell lymphoma. Patients who developed either disease progression or a partial response 3 months following axicabtagene ciloleucel CAR T-cell infusion were found to have enrichment of exhausted CD8<sup>+</sup> T cells (95). In contrast, and reciprocally, those with complete response were enriched with memory CD8<sup>+</sup> T cells in preinfusion anti-CD19 CAR T cells. These data suggests that improved CAR T-cell efficacy may be achieved by enriching for CD8<sup>+</sup> CAR T cells with a memory gene signature.

Another promising example has been observed for HER2<sup>+</sup> breast cancers that are unresponsive to anti-HER2-directed therapy and CDK4/6 inhibitors, both routinely utilized as a standard-of-care treatment and investigated in clinical trials as a promising combination for treating HER2<sup>+</sup> breast cancers. In an effort to use scRNA-seq for patient-guided immunotherapeutic intervention, investigators identified an infiltrated immunosuppressive myeloid cell population that conferred resistance to treatment with trastuzumab and palbociclib (96). Guided by scRNA-seq analyses, combination treatment with cabozantinib, a tyrosine kinase inhibitor with activity against upregulated target genes seen in immunosuppressive myeloid cells, overcame resistance and further sensitized tumors to immune checkpoint blockade. Thus, in a variety of cancers, scRNA-seq serves as a formidable platform to completely deconstruct the TME to discover novel and efficacious immunotherapies. Though there are certain limitations, including intrinsically noisy data due to transcriptional burst-like stochastic pulses (97, 98), leading to ambiguous or false-negative results, pathway enrichment analyses can overcome these issues. Another area for improvement comes from the difficulty in establishing correlations between genotype and phenotype due to technical limitations for confidently resolving tumoral copy-number variations and somatic single-nucleotide variants (99). In addition to the inherent cellular limitations of scRNA-seq, issues with sample procurement and processing can also challenge data interpretation. Whereas the peripheral blood or lymph can offer ready single-cell suspensions for scRNA-seq, processing time ahead of cryopreservation can significantly impact the data (100). This is even more challenging when scRNA-seq is used on cells obtained from solid tumor tissues as a result of differences in dissociation methods and cryopreservation conditions (101).

Such issues, in addition to other challenges with this technology (73), will greatly benefit from the introduction of more highly standardized techniques for tissue dissociation and cell suspension preparation of single-cell suspensions (102), in which single-nucleus RNA-seq (snRNA-seq) may substantially improve the characterizing of single-cell atlases and clinical utility of this technology (103, 104), in addition to the introduction of new standardized methods to correct for batch effects (105), which will also aid single-cell

research in other IO-relevant areas, including genomics, proteomics, and epigenetics (106–108). Of note, computational methods for the spatial reconstruction of TMEs from scRNA-seq data (109), in addition to advancements of scRNA-seq methods for use on frozen specimens and FFPE tissues (110, 111), are gaining pace for generation of comprehensive cellular atlases of pan-cancer TMEs and the implementation of scRNA-seq into clinical practice.

### Visium spatial gene expression: barcoding transcriptomes across TMEs

Although the power of single-cell transcriptomics has enabled high-dimensional gene profiling of immune cells (31) and high-resolution characterization of a much greater number of immune cell subsets than previously appreciated (32), this technology still has room for improvement. Low capture efficiency and sequencing coverage and a high rate of dropout events can complicate the ease of the study of cell-cell interaction and higher-order tissue structures influencing or impeding immunity (33, 34, 112).

Enter the field of spatial genomics by a company appropriately named “Spatial Transcriptomics” (ST) pioneered in 2016 by Ståhl and colleagues (113), a technique enabling quantitative visualization and analysis of the transcriptome within intact tissue sections via unique spatially barcoded oligodeoxythymidine microarrays, as introduced to preserve spatial positioning within tissue architectures prior to RNA-seq. This important method has its basis in various forms of historic uses of *in situ* hybridization (ISH) used for many years to visualize spatiotemporal gene expression, beginning with radioactive ISH in 1969 by Gall and John to observe ribosomal RNA (114) and DNA (115) and then to see specific gene transcripts by Harrison (116). Nonradioactive fluorescent and colorimetric ISH improving spatial resolution, enabling 3D staining, and shortening of exposure times was then developed by Langer-Safer and colleagues (117) and Rudkin and colleagues (118), whereas whole mount ISH was introduced by Tautz and colleagues (119), followed by the development of reference databases by the first DNA screens (120–122). After a few additional key historic inventions (reviewed in ref. 123) leading to ST development, and including the first unequivocal demonstration of single-molecule FISH in 1998 by Femino and colleagues (124), ST analyses of pancreatic, breast, prostate, and melanoma specimens have revealed unprecedented observations of intratumoral and intertumoral heterogeneity and gene expression difference between tumor and peripheral material (113, 125, 126) using multimodal intersection analysis to produce an unbiased RNA-seq map of cellular transcripts across tissues (127).

ST was acquired by 10x Genomics in 2018 and rereleased as the Visium Spatial Gene Expression (SGE) Solution with higher resolution and increased sensitivity, heralded as method of the year (128). The most widely used generation of SGE for FFPE or fresh-frozen tissue contains four 6.5 × 6.5 mm tissue capture areas per slide, and each tissue capture area contains 5,000 × 55 μm diameter spots containing oligonucleotide barcodes covalently attached to the Visium SGE slide. For Visium SGE, 10-μm-thick tissue sections are placed in each tissue capture area, and hematoxylin and eosin IHC staining is then performed, following an enzymatic permeabilization of the tissue. The 3' poly-A tail of exposed mRNA hybridizes to the 5' poly-T of the barcodes, and the nucleotides are amplified and mapped back to genes in a reference genome and to a spot on the slide. The readout produces the hematoxylin and eosin- or IHC-stained tissue image overlaid with the genome-wide mRNA molecular count per gene of the cellular content contained in each

55  $\mu\text{m}$  spot and the geometric coordinates of the spot within the tissue capture area.

One application of Visium SGE has been to characterize heterogeneity within TMEs, including niches of interacting cells and cellular composition at the leading edge of tumors (129). Another application has focused on tertiary lymphoid structures, which are immune aggregates in tumors and peripheral tissue that form under chronic inflammatory states (130–132). Visium SGE has enabled the identification of various B-cell maturation states within tertiary lymphoid structures, including clonotype expanded populations found in tumors using a modified Visium SGE protocol for B-cell receptor sequencing (132). Visium SGE has further been paired with pooled CRISPR screens to spatially resolve genetic contributors to the TME in mouse models, such as identifying differential roles of TGF- $\beta$  in cancer cells versus fibroblasts elucidated using Perturb-map (133).

A major challenge in the current use of Visium SGE is that it does not have single-cell resolution (123). That is, a 55  $\mu\text{m}$  diameter spot with 10- $\mu\text{m}$ -thick tissue is estimated to contain 1 to 10 cells per spot on average, but dense immune aggregates may contain upward of 30 to 50 cells per spot, making cellular resolution difficult, and thus challenging collected insight for many studies. Several deconvolution methods have been developed to computationally infer cellular resolution information from Visium by coupling it with single-cell transcriptomics (134–138). The most recently released 10X Genomics Visium HD, however, has the potential to overcome resolution issues, boasting a continuous grid-pattern of  $2 \times 2 \mu\text{m}$  squares (i.e., more than half the size of a typical cell), and is able to detect 11 million features for each square for sub-single cell-scale gene expression resolution (139).

Other competing or complementing multiple spatial transcriptomics platforms are continually being developed in parallel to Visium technology, including the NanoString GeoMx Digital Spatial Profiler (DSP) that provides RNA expression by stratifying cells within user-defined regions of interest (ROI) according to protein markers [see resource (140)]. The platform enables ROI selection along a considerably larger tissue, enabling better assessment of heterogeneity within tumor lesions. Several other ISH spatial transcriptomics techniques are also commercially available, including MERFISH and Slide-seqV2, having a spatial resolution of 10  $\mu\text{m}$  (141), enabling subcellular spatial information of transcripts. Whereas the resolution offered by other technologies still currently surpass that of validated Visium SGE, the libraries involve targeted probes for each gene with different hybridization affinities. This is mitigated by the Visium SGE platform because all genes are captured by hybridization at the common 3' poly-A tail of each transcript.

#### **GeoMx: protein and transcriptome barcoding TMEs**

Whereas other tissue-based spatial transcriptomics are able to measure the expression profile of many genes simultaneously, gene expression does not necessarily equate protein expression. In addition, whereas gene expression panels are interesting, a true biomarker usually still needs to be validated at the levels of protein expression and function. The GeoMx DSP was revolutionary since its release by NanoString in 2019 because it could read both RNA and protein. This platform is a reagent, an instrument, and a software system that enables high-plex assessment of transcripts (>18,000 genes) and/or proteins (>100 proteins) in a single tissue (142). GeoMx can be used on both FFPE and fresh-frozen tissues. The GeoMx platform's interactive software allows for collaboration between pathologists, researchers, and analysts through a remote interface. GeoMx procedures are similar to traditional IHC and ISH protocols. During the procedure, the hybridization of the UV photocleavable linked mRNA probes or antibodies used for target

detection and fluorescent visualization reagents are performed simultaneously. The following day, the GeoMx instrument scans the fluorescent images to visualize the tissue architecture, and ROIs ranging in size from  $5 \times 5 \mu\text{m}$  up to  $660 \times 785 \mu\text{m}$  can be selected by the user. ROIs can be further subdivided into areas of illumination (AOI) with a resolution down to 1  $\mu\text{m}$  using binary masks as defined by the pattern of one or more of the fluorescent channels. AOIs can be irregular shapes, noncontiguous segments, or a specific cell type such as tumor or immune. Following AOI selection, the DSP instrument directs UV light to the specific AOI, in which the UV photocleavable linker is severed, and the oligonucleotide tags are released and collected for off-instrument quantitation. Digital counts are mapped back to the tissue location in the DSP software, resulting in a spatially resolved digital profile of protein or mRNA abundance for each AOI.

One advantage of the GeoMx platform is the ability to profile RNA transcripts and proteins based on the geography of the tissue. Fluorescent morphology markers are used to visualize intrinsic tissue structures, such as the tumor epithelium [e.g., pan-cytokeratin (panCK)] or specific immune cell types (e.g., CD45, all leukocytes; CD3, all T cells). This allows for the characterization of specific immune compartments within TMEs. A common use for this is profiling immunity within the tumor epithelium versus the tumor stroma, in which a pathologist places ROIs in tumor regions and then defines AOIs within these ROIs (e.g., based on panCK-positive tumor and panCK-negative stroma) and collects separately to search for biomarkers emanating from separate compartments. This particular analysis of immune infiltration in the tumor versus stroma compartment permits the identification of protein and transcriptomic biomarkers that identify factors related to areas of interest, including lymphocyte exclusion or mechanisms of resistance to immunotherapy (143, 144).

The application of GeoMx for profiling either in archival and biopsy tumor tissues has been shown for several different tumor indications in which novel biomarkers correlating with response to immunotherapies have been found. In examining the CD45-immune compartment in tumors from patients with non-small cell lung cancer (NSCLC) treated with anti-PD-1 therapy, high levels of CD56 and CD4 markers were predictive for all clinical outcomes (145). Multiple groups have shown that in triple-negative breast cancer, colorectal cancer, NSCLC, and melanoma, GeoMx-based PD-L1 protein quantification is concordant with standard PD-L1 IHC and correlates with response to immunotherapy (144, 146–148). Similarly, GeoMx has identified molecular pathways related to fibroblasts in head and neck cancers, Notch signaling in small cell lung cancer (149), immune signaling in metastatic disease (150), and immune activation markers in glioblastoma (151), and as correlating with response or resistance to checkpoint inhibitors and combination therapy. Preclinical studies using GeoMx have also shown detection of biological mechanisms and biomarkers of response in lung and bladder cancer models (152).

Detection of biomarkers for immunotherapy by GeoMx has not only been limited to checkpoint inhibitors. Biomarkers in response to bispecific antibody therapy in bone marrow biopsies from patients with acute myeloid leukemia have also been identified (153). GeoMx has also been used to detect biomarkers related to response to cellular immunotherapy using both CAR T cells (NCT03089203) and transgenic T cells (154, 155). GeoMx is a key platform for biomarker discovery in clinical samples both because of its optimal performance in FFPE samples and its ability to easily quantify both proteins and RNA transcripts within a single slide and with very small amounts of tissue.

Although this technology is gaining broad acceptance by the clinical community, there are also several spatial transcriptomic platforms in various levels of development that have a different functionality than GeoMx. When profiling large tissues, it can become expensive to profile ROIs from an entire tissue. Whole tissue analysis is more easily done using Visium or PhenoCycler-Fusion, which profiles the entire slide. Additionally, GeoMx does not have single-cell or subcellular resolution. Therefore, platforms such as Visium HD, PhenoCycler-Fusion, and CosMx spatial molecular imaging may be better options for single-cell scale resolution.

### Spatially resolved proteomics: mass spectrometry imaging and related technologies

Mass spectrometry imaging (MSImg) is a powerful label-free imaging technique that enables *in situ* evaluation of the spatial proteome, lipidome, glycane, and metabolome in tissue sections. It is becoming increasingly popular for the discovery of biomarkers (156, 157). As an emerging technology, MSImg utilizes the multiplexed measurement capability of mass spectrometers combined with a surface scanning sampling process that allows one to rapidly detect and map endogenous and exogenous compounds from a single tissue sample or a series of tissue sections into 2D or 3D optical images (158). During the last decade, MSImg has emerged as a promising technique and it is beginning to show enormous potential to provide new insights into the basic/clinic medical sciences (159, 160), owing to its unique ability to acquire molecular-specific images and to provide information on many hundreds of molecular ions, without the need for specific staining or labeling, in contrast to other commonly used visualization methods (e.g., IHC, IF, or radioimmunoassay).

To date, secondary ion MSImg (SIMSI), desorption electrospray ionization MSImg (DESI-MSI), and matrix-assisted laser desorption/ionization MSImg (MALDI-MSI) are three well-established MSImg techniques (161, 162). Among these, SIMSI, representing the earliest MSImg technique developed in the 1980s, can provide very high spatial resolution with typical scanning step sizes from tens to hundreds of nanometers (163). Because the high energy of the primary ion beam used in SIMSI is higher than the energy of the covalent bonds within endogenous and exogenous compounds, this technique always leads to the extensive fragmentation of molecules during surface ionization, resulting in a detectable mass range limitation of below 1,000 Da. Although SIMSI is not compatible with the characterization of large molecular compounds (such as proteins), it has been widely used in the screening of small molecular markers (such as lipids, small molecular metabolites, and elements) and in the characterization of drug molecules with high spatial resolution (164–168). DESI-MSI was successfully developed by Cooks' group (169, 170) in the early part of the 21st century. DESI-MSI utilizes tiny, charged droplets generated by an electrospray ionization (ESI) liquid-flow source to collide with and touch the surface of a tissue sample to achieve the dissolution, desorption, and high-efficiency ionization of analytes, which subsequently enter a high-performance mass spectrometer for analysis. To overcome ESI jet-focusing limitations, DESI-MSI enables mapping and quantification of compounds present in the tissue surface with a spatial resolution of approximately 50 to 200 μm (171, 172). DESI-MSI, it should be noted, as one of the ambient ionization MSImg techniques, allows the rapid analysis of analytes in tissue samples in their original states and is very suitable for the rapid analysis of large samples, enabling the possibility of "online living analysis" or "real-time diagnosis or surgery" (173–175). DESI-MSI has already been widely used in the medical sciences, playing an important role in the

screening and discovery of novel biomarkers, the study of disease pathogenesis, the development of new drugs, and the monitoring of drug delivery and tracing (176, 177).

MALDI-MSI was first described in 1994 during the 42nd American Society for Mass Spectrometry Conference by Bernhard Spengler and was later further developed in 1997 by Caprioli's group (178). MALDI-MSI is well-positioned to overcome the challenges of intact protein detection and imaging by SIMSI and DESI-MSI. The latest studies from Wang's group show that MALDI-MSI can directly detect and image proteins with an upper molecular weight limit up to 200,000 Da (179). MALDI-MSI is arguably the most versatile "soft" ionization platform, combining relative high lateral resolution (1.4–10 μm; refs. 180, 181), wide detectable mass range (0–200,000 Da; ref. 179), high speed (laser frequency up to 10 kHz; ref. 182), and the ability to combine the molecular specificity of MALDI-MS detection with spatial distribution information (156, 157), which has led to the technique being extensively used within many medical science fields, such as biomarker discovery, disease diagnosis, tumor typing, drug distribution mapping, and others (183–185).

The rapid development of sample preparation methods (e.g., matrix coating assisted by an electric field on-tissue chemical derivatization; refs. 186, 187), new MALDI matrix screening [(e.g., "green" organic acid matrices (188, 189)], nanoparticle matrices, and new ionization technologies [(e.g., MALDI combined with laser-induced postionization, MALDI-2 (190–192)], ambient infrared MALDI, IR-MALDI (193–195), improvements in instrument mass analyzer technology [(e.g., trapped ion mobility spectrometry (196, 197)], greatly enhanced MALDI-MSI's increasingly wide applications in medical science, particularly in biomarker screening and discovery. It can be predicted that accurate *in situ* detection and imaging of new biomarkers based on single-cell spatial multi-omics, rapid online living analysis, and real-time precision assisted surgery will be important leading edges of MSImg.

### Bulk proteomics: from discovery to quantitation by MS

As discussed earlier, MS-based proteomic methods distinguish themselves from other methods as they do not rely on any types of probes (e.g., antibodies or aptamers) for identifying and quantifying the protein of interest. Instead, the mass-to-charge ratio ( $m/z$ ) signal obtained from the protein itself or a proteotypic surrogate peptide is used. Although it sometimes comes at the cost of spatial distribution, these technologies avoid some of the pitfalls of antibodies: the lack of specificity, selectivity, reproducibility, or standardization. MS-based workflows can be either untargeted or targeted approaches, both of which are detailed in Sobsey and colleagues (198).

Following the development of electrospray for protein analysis in 1989 by Fenn and colleagues (199), MS-based technologies have been continuously refined and boosted in their sensitivities and speed, nowadays permitting a truly in-depth characterization of the entire proteome, in which as little as 10 ng of sample can be used for deep proteome coverage by LC-MS (refs. 200, 201). The fact that this is within the range of the amount of protein content per cell, (202, 203), with typical per cell proteomes consisting of ~12,000 proteins (204), has spurred a new quest for robust measurement of single-cell proteomes (205). Similar technologies such as single-cell proteomics by mass spectrometry (ref. 206) and Nanodroplet Processing in One Pot for Trace Samples (refs. 207, 208) also provide in-depth proteome coverage.

The identification of proteomics-based predictive biomarkers for response to IO therapy has been considered the holy grail of

oncology biomarkers by this field for several years, despite it not having yet provided robust enough biomarkers with the power to alter clinical practices. In melanoma, comparative studies of IO responders versus nonresponders highlight inherent differences in metabolism with better outcomes for patients with higher expression of proteins related to mitochondrial metabolism (209, 210). NLRC5 and STAT1 were also reported as relevant predictors of IO therapeutic response in relation to metabolism regulation (209), whereas others have identified a direct correlation between neutrophil defensin 1, 2, and 3 protein expression with IO responses using MALDI imaging (211). Although some groups have presented proteomic signatures associated with IO responses (210, 212), the complexity of the required workflow is better suited for hypothesis generation and discovery-based programs than for large-scale clinical testing. Clinical practice requires reproducibility and standardization which is often difficult to obtain with nontargeted methods.

In contrast to untargeted approaches providing relative quantification, targeted proteomics approaches integrate the high selectivity and specificity of MS with the well-established robustness of clinical chemistry. These assays generally use stable isotope-labeled standard peptides or proteins spiked in at a known concentration and can monitor anywhere from one to 100 of proteins within one experiment to report an “absolute” concentration of each target (e.g., fmol/μg or pg of protein per μg of total protein or mg of tissue). Thus far, all targeted MS-based assays for immunotherapy have included PD-L1 and PD-1, sometimes adding a combination of related markers like PD-L2 and IDO1 (213–218). These studies have confirmed that the detection of PD-L1 by IHC is affected by its N-glycosylation (215), FFPE storage time, experimental conditions, and IHC kits (22C3, 28-8, E1L3N, and SP142), whereas MS-based methods remained unaffected by these issues (213). However, none of these studies have managed to test these assays on IO-treated patients, nor were they able to assess the test’s clinical utility. Whiteaker and colleagues (216) have recently proposed a highly multiplexed (46 proteins, including PD-L1 and PD-L2) assay based on an antipeptide immune enrichment followed by MS-based targeted analysis. Similarly, Lacasse and colleagues (219) proposed an “immunoscore” based on the quantification of PD-L1, PD-L2, PD-1, LCK, ZAP70, and NT5E, which has already shown its potential prognostic value in NSCLC and is currently validating its clinical utility in ICI-treated patients. Unlike antiprotein antibodies, peptide antibodies offer a more reliable recovery, are unaffected by structural changes in target proteins, and can also be designed to avoid or measure posttranslational modifications (refs. 198, 220). Whiteaker and colleagues’ (216) work is of special interest as it has been validated for plasma, fresh-frozen, and FFPE tissues. Ibrahim and colleagues also proposed an interesting alternative to the time-consuming calibration curves using two peptide isotopologues internal standards, allowing internal calibration which decreases cost, time, and the matrix effect (220, 221).

Thus far, although MS-based methods in tissues hold a great deal of promise, like other technologies discussed, their developments have been challenged by the inaccessibility of IO-treated patient samples. Numerous other MS-based methods’ experimental and analytical limitations and consideration have been described with published guidelines to overcome issues with tissue and matrix heterogeneity, ion suppression effects, and inefficient analyte recovery (222). Finally, however, whereas the details of the PELICAN study (NCT03515798) have not yet been made fully available, this IO breast cancer trial evaluating PD-L1 expression in pre-, per-, and

post-treatment tissues by both IHC and MS-based proteomics, in addition to PD-L1 expression in plasma using quantitative proteomics, will certainly shed some light on the benefits of MS-based quantification of proteins in IO settings.

## Best Biobanking Practices

Identifying reproducible and robust biomarkers of response, resistance, and toxicity to IO therapeutics using all the technologies outlined above has one common pitfall: They all heavily rely on the procurement and biobanking of high-quality biological specimens. The collection and processing of biospecimens must be performed following standard operating procedures to control for preanalytical variables, guaranteeing the quality of the materials to be analyzed and hence the reproducibility of the results obtained to facilitate future validation of biomarkers identified (223, 224). In fact, the presence of nonstandardized conditions for tissue collection, fixation, and processing of FFPE samples has contributed to the very challenging optimization and validation of PD-L1 assays for their mainstay in clinical practice (154). As learned from past trial experiences (e.g., NCT01276899), the pathologic evaluation of frozen or FFPE tissue specimens to determine the percentage of necrosis, stroma, and overall tumor cellularity is necessary to ensure the applicability of multi-omic analyses as these parameters can harshly impact DNA and RNA yields (225). It is therefore of critical importance to standardize and validate biospecimen practices for each individual type of biomarker in order to enable large-scale validation.

With the advent of immune-based therapies, biobanks are optimizing tumor collection and processing methods for more advanced genomic and functional immune analyses that have the potential to change the way we understand the TME in the face of IO. Groups must therefore adhere to SOPs for the collection and processing of fresh tumor specimens and the isolation of tumor infiltrating lymphocytes used for analyses, such as scRNA-seq allowing the characterization of tumor cells and immune cell states in IO response (226). The correct collection and dissociation of fresh lymph nodes immediately following surgery for flow cytometric and transcriptomic analyses has also provided a more detailed view of the immune cell composition of tumor lymph nodes and their impactful roles in IO response (227, 228).

The collection of serial samples to interrogate clinical and pharmacodynamic responses is crucial for IO discovery (229). This “next-generation biobanking” provides insights into tumor and immune system evolution over the course of specific therapies and may provide opportunities for modification of applied therapies or additional interventions. Harvesting tissue through serial biopsies or longitudinal blood samples requires important logistics that involve a multi-disciplinary team who takes part in obtaining patient consent and entering clinical data, identifying the appropriate lesion(s) and the timing of sample collection and then rapidly collecting and processing the samples and prioritizing the downstream analyses to be performed when limited patient tissue or blood is available (230). Recently, Yang and colleagues (231) have shown the potential of combining both serial tissue and liquid biopsy biomarkers to dynamically monitor IO treatment response to rule out tumor pseudoprogression and to identify biomarkers of resistance. Guidelines from biobanking institutions like the International Society for Biological and Environmental Repositories and others, aimed at creating policy for correct tissue processing methods for sample preservation and harmonization, should ultimately be considered during study design and correctly implemented to minimize sample variability within and across biomarker studies (232). These and

many new developments in refinement of harmonization of biobanking procedures will truly aid in bringing these biomarkers closer to clinical implementation.

## Conclusions and Perspectives

The single-cell profiling revolution has transformed biology, allowing researchers to investigate the genomics, transcriptomics, and epigenetics of the basic units of life (72). These approaches provide the power to build atlases of what multicellular organisms are made of for comparison against a confused or diseased state of the same cells populating the TME. However, this explosion in our understanding of tumor immunology came with great technical and biological limitations (233). The main technical limitations depend on the amount and type of information collected from either tissues or separated single cells. As a prominent example, RNA and DNA technologies are currently incompatible with the need to collect multiple samples per patient, which invariably increases the required sample volume and is not always feasible. Despite the reduction of sequencing costs, the price of single-cell technologies remains considerable and limits the number of samples per experiment, thus reducing power. Furthermore, the integration of diverse datasets is accompanied by data normalization and analysis challenges due to different sequencing chemistry and cell selection approaches (234). Current analysis and data processing platforms allow the exploration of single-cell data using a combination of supervised and unsupervised methods. Contrary to the few single-cell sequencing methods available, there is an abundance of analytic pipelines, and approaches are regularly published on a monthly basis, providing unparalleled flexibility in how to perform analysis (235). The next frontier involves the systematic combining of described approaches to understand and predict the behavior of complex systems such as cancer development, resistance, and metastasis. Another great barrier in single-cell biology is characterizing the relationship between single cells in tissues. Current methods such as VISIUM (236), PhenoCycler-Fusion (CODEX; ref. 237), Deep Visual Proteomics (ref. 238), MSImg (185), or GeoMx (236) can integrate next-generation sequencing and IHC by advancing further miniaturization and microfluidics. However, it is also possible to execute multiple assays in consecutive tissue blocks using technologies such as MICCSS or others (239) combined with single-cell sequencing and inference analysis (240).

The Cancer Immune Monitoring and Analysis Centers-Cancer Immunologic Data Commons Network, part of the NCI (<https://cimac-network.org/>), collaborates with more than 30 clinical trial teams, coordinating, collecting, and performing multiple cutting-edge assays to harness the capabilities of an anticancer immune response. This initiative has allowed the parallel collection of bulk, single-cell tissue, and liquid biopsies, allowing the parallel multi-omic analysis of assays such as RNA-seq (10 $\times$ , NanoString), proteomics (Olink), cellular components (CyTOF), tissue structure and composition (MICSS and mIHC), and more recently spatial transcriptomic and single-cell analyses (GeoMx, Visium SGE, and scRNA-seq). These trials, such as Hodgkin lymphoma (NCT01896999), recurrent metastatic endometrial cancer (NCT03367741), colorectal cancer (NCT02873195), NSCLC (NCT03451331), and others (NCT02978625, NCT04123379), can be integrated and analyzed using straightforward regression modeling strategies which allow a clear interpretation of the results (241). However, multifactorial and machine learning approaches such as random forest or neural networks can be applied to build prognostic or predictive models (242–244).

Our capacity to understand cancer biology has changed dramatically because of all of the advances made in fundamental sciences. There are still many improvements expected on the horizon, such as integrating tumor cell genetic heterogeneity with immune microenvironment diversity in a spatially resolved manner. This could lead to individual cell-cell interactions that are obscured by current methods without such granularity of data. Other examples of future developments will include the integration of tissue analyses with radiomics features in a 3D-aware fashion, as well as dynamics of spatial organization over time. These discovery tools will eventually require simplification if to be applied clinically, with a long way to go for biomarker implementation and usefulness. Nevertheless, the use of multi-omic strategies providing gene- and protein-level expression, the cell types present, what factors they are producing, and how they are interfering with immune response should provide new ways to both discover the true biomarkers of response and engineer cellular therapies that can better function in solid TMEs. Used in parallel, these approaches can direct the course of treatment for individual patients and improve our understanding of the yet unknown fundamentals of the interrelationship of IO and the host determinants of immune response (245). We are only now gaining a foothold of the true decision trees responding to the challenges surrounding the choice of the appropriate complimentary methods that need to be adopted when biospecimens and limited sample sizes prevent all possibly pertinent technologies from being used. The overarching promise of truly personalized cancer immunotherapies will greatly impact and extend overall health, quality of life, and survival of patients.

## Authors' Disclosures

P.K. Bommarddy reports other support from Replimmune Inc. outside the submitted work. D.L. Bonilla reports other support from Cytek Biosciences outside the submitted work and is currently the scientific director of Cytek Biosciences, Inc., a cytometer manufacturer. C.H. Borchers reports grants from Genome Canada and Genome BC during the conduct of the study as well as personal fees from MRM Proteomics, Inc. and Molecular You outside the submitted work; in addition, C.H. Borchers has a patent for US20170148618A1 issued. A.P. Cogdill reports personal fees from Daiichi Sankyo and Immunati outside the submitted work. N. Hacohen reports grants from Bristol Myers Squibb and Calico Life Sciences and personal fees from CytoReason, Repertoire Immune Medicines, and Danger Bio/Related Sciences outside the submitted work. V. Lacasse reports a patent for MRMP-0001PUSN pending. W.-R. Lie reports other support from Millipore Sigma during the conduct of the study and outside the submitted work. A. Mehta reports personal fees from Third Rock Ventures, personal fees and other support from Asher Biotherapeutics and Abata Therapeutics, and other support from Clasp Therapeutics outside the submitted work. A. Spatz reports grants and personal fees from Pfizer and AstraZeneca and personal fees from Amgen, Janssen, Bristol Myers Squibb, and Roche outside the submitted work. B. Taouli reports grants and personal fees from Bayer and Guerbet, personal fees from Ascelia, grants from Takeda and Regeneron, and nonfinancial support from Echosens outside the submitted work. I. Tirosh is an advisory board member of Immunitas Therapeutics. S. Gnjatic reports grants from Regeneron, Boehringer Ingelheim, Janssen R&D, Genentech, Takeda, Bristol Myers Squibb, and Celgene and personal fees from Taiho Pharmaceuticals outside the submitted work; in addition, S. Gnjatic has a patent for MICSS issued and a patent for NY-ESO-1 Polypeptides issued. No disclosures were reported by the other authors.

## Acknowledgments

The authors acknowledge Society for Immunotherapy of Cancer staff for their contributions, including Flynn DeWalt, Ellie Rickman, and Peter Intile, PhD, for support, project management, and editorial assistance. Additionally, the authors wish to thank the society for supporting the development of the manuscript.

Received July 31, 2024; revised September 27, 2024; accepted November 12, 2024; published first December 3, 2024.

## References

- Sharma P, Wagner K, Wolchok JD, Allison JP. Novel cancer immunotherapy agents with survival benefit: recent successes and next steps. *Nat Rev Cancer* 2011;11:805–12.
- Mahoney KM, Freeman GJ, McDermott DF. The next immune-checkpoint inhibitors: PD-1/PD-L1 blockade in melanoma. *Clin Ther* 2015;37:764–82.
- Vaddepally RK, Kharel P, Pandey R, Garje R, Chandra AB. Review of indications of FDA-approved immune checkpoint inhibitors per NCCN guidelines with the level of evidence. *Cancers (Basel)* 2020;12:738.
- Karasarides M, Cogdill AP, Robbins PB, Bowden M, Burton EM, Butterfield LH, et al. Hallmarks of resistance to immune-checkpoint inhibitors. *Cancer Immunol Res* 2022;10:372–83.
- Saez-Ibanez AR, Upadhyaya S, Campbell J. Immuno-oncology clinical trials take a turn beyond PD1/PDL1 inhibitors. *Nat Rev Drug Discov* 2023;22:442–3.
- Dong H, Strome SE, Salomao DR, Tamura H, Hirano F, Flies DB, et al. Tumor-associated B7-H1 promotes T-cell apoptosis: a potential mechanism of immune evasion. *Nat Med* 2002;8:793–800.
- Patel SP, Kurzrock R. PD-L1 expression as a predictive biomarker in cancer immunotherapy. *Mol Cancer Ther* 2015;14:847–56.
- Sul J, Blumenthal GM, Jiang X, He K, Keegan P, Pazdur R. FDA approval summary: pembrolizumab for the treatment of patients with metastatic non-small cell lung cancer whose tumors express programmed death-ligand 1. *Oncologist* 2016;21:643–50.
- Llosa NJ, Cruise M, Tam A, Wicks EC, Hechenbleikner EM, Taube JM, et al. The vigorous immune microenvironment of microsatellite instable colon cancer is balanced by multiple counter-inhibitory checkpoints. *Cancer Discov* 2015;5:43–51.
- Marcus L, Fashoyin-Aje LA, Donoghue M, Yuan M, Rodriguez L, Gallagher PS, et al. FDA approval summary: pembrolizumab for the treatment of tumor mutational burden-high solid tumors. *Clin Cancer Res* 2021;27:4685–9.
- Marcus L, Lemery SJ, Keegan P, Pazdur R. FDA approval summary: pembrolizumab for the treatment of microsatellite instability-high solid tumors. *Clin Cancer Res* 2019;25:3753–8.
- Parsons R, Li GM, Longley MJ, Fang WH, Papadopoulos N, Jen J, et al. Hypermutability and mismatch repair deficiency in RER<sup>+</sup> tumor cells. *Cell* 1993;75:1227–36.
- Doroshow DB, Bhalla S, Beasley MB, Sholl LM, Kerr KM, Gnjatic S, et al. PD-L1 as a biomarker of response to immune-checkpoint inhibitors. *Nat Rev Clin Oncol* 2021;18:345–62.
- Goodman AM, Sokol ES, Frampton GM, Lippman SM, Kurzrock R. Microsatellite-stable tumors with high mutational burden benefit from immunotherapy. *Cancer Immunol Res* 2019;7:1570–3.
- Li K, Luo H, Huang L, Luo H, Zhu X. Microsatellite instability: a review of what the oncologist should know. *Cancer Cell Int* 2020;20:16.
- Merino DM, McShane LM, Fabrizio D, Funari V, Chen S-J, White JR, et al. Establishing guidelines to harmonize tumor mutational burden (TMB): in silico assessment of variation in TMB quantification across diagnostic platforms: phase I of the Friends of Cancer Research TMB Harmonization Project. *J Immunother Cancer* 2020;8:e000147.
- Sha D, Jin Z, Budczies J, Kluck K, Stenzinger A, Sinicrope FA. Tumor mutational burden as a predictive biomarker in solid tumors. *Cancer Discov* 2020;10:1808–25.
- Vega DM, Yee LM, McShane LM, Williams PM, Chen L, Vilimas T, et al. Aligning tumor mutational burden (TMB) quantification across diagnostic platforms: phase II of the Friends of Cancer Research TMB Harmonization Project. *Ann Oncol* 2021;32:1626–36.
- Gaule P, Smith JW, Toki M, Rehman J, Patell-Socha F, Cougot D, et al. A quantitative comparison of antibodies to programmed cell death 1 ligand 1. *JAMA Oncol* 2017;3:256–9.
- Rimm DL, Han G, Taube JM, Yi ES, Bridge JA, Flieder DB, et al. A prospective, multi-institutional, pathologist-based assessment of 4 immunohistochemistry assays for PD-L1 expression in non-small cell lung cancer. *JAMA Oncol* 2017;3:1051–8.
- Rutella S, Cannarile MA, Gnjatic S, Gomes B, Guinney J, Karanikas V, et al. Society for Immunotherapy of Cancer clinical and biomarkers data sharing resource document: volume I-conceptual challenges. *J Immunother Cancer* 2020;8:e001389.
- Cesano A, Cannarile MA, Gnjatic S, Gomes B, Guinney J, Karanikas V, et al. Society for Immunotherapy of Cancer clinical and biomarkers data sharing resource document: volume II-practical challenges. *J Immunother Cancer* 2020;8:e001472.
- Helmink BA, Reddy SM, Gao J, Zhang S, Basar R, Thakur R, et al. B cells and tertiary lymphoid structures promote immunotherapy response. *Nature* 2020;577:549–55.
- Davis MM, Tato CM, Furman D. Systems immunology: just getting started. *Nat Immunol* 2017;18:725–32.
- Romero P, Banchereau J, Bhardwaj N, Cockett M, Disis ML, Dranoff G, et al. The Human Vaccines Project: a roadmap for cancer vaccine development. *Sci Transl Med* 2016;8:334ps9.
- Rozenblatt-Rosen O, Regev A, Oberdoerffer P, Nawy T, Hupalowska A, Rood JE, et al. The human tumor atlas network: charting tumor transitions across space and time at single-cell resolution. *Cell* 2020;181:236–49.
- Thorsson V, Gibbs DL, Brown SD, Wolf D, Bortone DS, Ou Yang T-H, et al. The immune landscape of cancer. *Immunity* 2019;51:411–2.
- Thorsson V, Gibbs DL, Brown SD, Wolf D, Bortone DS, Ou Yang T-H, et al. The immune landscape of cancer. *Immunity* 2018;48:812–30.e14.
- Stanta G, Bonin S. Overview on clinical relevance of intra-tumor heterogeneity. *Front Med (Lausanne)* 2018;5:85.
- Gibbs DL, Aguilar B, Thorsson V, Ratushny AV, Shmulevich I. Patient-specific cell communication networks associate with disease progression in cancer. *Front Genet* 2021;12:667382.
- Leader AM, Grout JA, Maier BB, Nabet BY, Park MD, Tabachnikova A, et al. Single-cell analysis of human non-small cell lung cancer lesions refines tumor classification and patient stratification. *Cancer Cell* 2021;39:1594–609.e12.
- Zheng L, Qin S, Si W, Wang A, Xing B, Gao R, et al. Pan-cancer single-cell landscape of tumor-infiltrating T cells. *Science* 2021;374:abe6474.
- Henke E, Nandigama R, Ergün S. Extracellular matrix in the tumor microenvironment and its impact on cancer therapy. *Front Mol Biosci* 2019;6:160.
- Nishida-Aoki N, Gujrati TS. Emerging approaches to study cell-cell interactions in tumor microenvironment. *Oncotarget* 2019;10:785–97.
- Hoyt CC. Multiplex immunofluorescence and multispectral imaging: forming the basis of a clinical test platform for immuno-oncology. *Front Mol Biosci* 2021;8:674747.
- Tan WCC, Nerurkar SN, Cai HY, Ng HHM, Wu D, Wee YTF, et al. Overview of multiplex immunohistochemistry/immunofluorescence techniques in the era of cancer immunotherapy. *Cancer Commun (Lond)* 2020;40:135–53.
- Taube JM, Akturk G, Angelo M, Engle EL, Gnjatic S, Greenbaum S, et al. The Society for Immunotherapy of Cancer statement on best practices for multiplex immunohistochemistry (IHC) and immunofluorescence (IF) staining and validation. *J Immunother Cancer* 2020;8:e000155.
- Asp M, Bergenstråhl J, Lundeberg J. Spatially resolved transcriptomes-next generation tools for tissue exploration. *Bioessays* 2020;42:e1900221.
- Heidelberger M, Kendall FE, Soo Hoo CM. Quantitative studies on the precipitin reaction: antibody production in rabbits injected with an azo protein. *J Exp Med* 1933;58:137–52.
- Marrack J. Nature of antibodies. *Nature* 1934;133:292–3.
- Coons AH, Creech HJ, Jones RN. Immunological properties of an antibody containing a fluorescent group. *Proc Soc Exp Biol Med* 1941;47:200–2.
- Nakane PK, Pierce GB Jr. Enzyme-labeled antibodies: preparation and application for the localization of antigens. *J Histochem Cytochem* 1966;14:929–31.
- Sternberger LA, Hardy PH Jr, Cuculis JJ, Meyer HG. The unlabeled antibody enzyme method of immunohistochemistry preparation and properties of soluble antigen-antibody complex (horseradish peroxidase-antihorseradish peroxidase) and its use in identification of spirochetes. *J Histochem Cytochem* 1970;18:315–33.
- Mason DY, Sammons R. Alkaline phosphatase and peroxidase for double immunoenzymatic labelling of cellular constituents. *J Clin Pathol* 1978;31:454–60.
- Singer SJ. Preparation of an electron-dense antibody conjugate. *Nature* 1959;183:1523–4.
- Faulk WP, Taylor GM. An immunocolloid method for the electron microscope. *Immunochimistry* 1971;8:1081–3.
- Huang SN, Minassian H, More JD. Application of immunofluorescent staining on paraffin sections improved by trypsin digestion. *Lab Invest* 1976;35:383–90.
- Hsu SM, Raine L. Protein A, avidin, and biotin in immunohistochemistry. *J Histochem Cytochem* 1981;29:1349–53.

49. Bodey B. The significance of immunohistochemistry in the diagnosis and therapy of neoplasms. *Expert Opin Biol Ther* 2002;2:371–93.
50. Leong AS, Wright J. The contribution of immunohistochemical staining in tumour diagnosis. *Histopathology* 1987;11:1295–305.
51. Nadji M. Immunoperoxidase techniques. I. facts and artifacts. *Am J Dermatopathol* 1986;8:32–6.
52. Swanson PE. HIERanarchy: the state of the art in immunohistochemistry. *Am J Clin Pathol* 1997;107:139–40.
53. de Matos LL, Trufelli DC, de Matos MGL, da Silva Pinhal MA. Immunohistochemistry as an important tool in biomarkers detection and clinical practice. *Biomark Insights* 2010;5:9–20.
54. Lu S, Stein JE, Rimm DL, Wang DW, Bell JM, Johnson DB, et al. Comparison of biomarker modalities for predicting response to PD-1/PD-L1 checkpoint blockade: a systematic review and meta-analysis. *JAMA Oncol* 2019;5:1195–204.
55. Taube JM, Roman K, Engle EL, Wang C, Ballesteros-Merino C, Jensen SM, et al. Multi-institutional TSA-amplified Multiplexed Immunofluorescence Reproducibility Evaluation (MITRE) Study. *J Immunother Cancer* 2021;9:e002197.
56. Parra ER, Uraoka N, Jiang M, Cook P, Gibbons D, Forget M-A, et al. Validation of multiplex immunofluorescence panels using multispectral microscopy for immune-profiling of formalin-fixed and paraffin-embedded human tumor tissues. *Sci Rep* 2017;7:13380.
57. Surace M, DaCosta K, Huntley A, Zhao W, Bagnall C, Brown C, et al. Automated multiplex immunofluorescence panel for immuno-oncology studies on formalin-fixed carcinoma tissue specimens. *J Vis Exp* 2019;143:e58390.
58. Chattopadhyay PK, Roederer M. Cytometry: today's technology and tomorrow's horizons. *Methods* 2012;57:251–8.
59. Parra ER, Jiang M, Solis L, Mino B, Laberiano C, Hernandez S, et al. Procedural requirements and recommendations for multiplex immunofluorescence tyramide signal amplification assays to support translational oncology studies. *Cancers (Basel)* 2020;12:255.
60. Barua S, Solis L, Parra ER, Uraoka N, Jiang M, Wang H, et al. A functional spatial analysis platform for discovery of immunological interactions predictive of low-grade to high-grade transition of pancreatic intraductal papillary mucinous neoplasms. *Cancer Inform* 2018;17:1176935118782880.
61. Johnson DB, Bordeaux J, Kim JY, Vaupel C, Rimm DL, Ho TH, et al. Quantitative spatial profiling of PD-1/PD-L1 interaction and HLA-DR/IDO-1 predicts improved outcomes of anti-PD-1 therapies in metastatic melanoma. *Clin Cancer Res* 2018;24:5250–60.
62. Berry S, Giraldo NA, Green BF, Cottrell TR, Stein JE, Engle EL, et al. Analysis of multispectral imaging with the AstroPath platform informs efficacy of PD-1 blockade. *Science* 2021;372:ea62609.
63. Goltsev Y, Samusik N, Kennedy-Darling J, Bhate S, Hale M, Vazquez G, et al. Deep profiling of mouse splenic architecture with CODEX multiplexed imaging. *Cell* 2018;174:968–81.e15.
64. Black S, Phillips D, Hickey JW, Kennedy-Darling J, Venkataraman VG, Samusik N, et al. CODEX multiplexed tissue imaging with DNA-conjugated antibodies. *Nat Protoc* 2021;16:3802–35.
65. Phillips D, Schürch CM, Khodadoust MS, Kim YH, Nolan GP, Jiang S. Highly multiplexed phenotyping of immunoregulatory proteins in the tumor microenvironment by CODEX tissue imaging. *Front Immunol* 2021;12:687673.
66. Jhaveri N, Ben Cheikh B, Nikulina N, Ma N, Klymyshyn D, DeRosa J, et al. Mapping the spatial proteome of head and neck tumors: key immune mediators and metabolic determinants in the tumor microenvironment. *GEN Biotechnol* 2023;2:418–34.
67. Khodadoust MS, Rook AH, Porcu P, Foss F, Moskowitz AJ, Shustov A, et al. Pembrolizumab in relapsed and refractory mycosis fungoides and sézary syndrome: a multicenter phase II study. *J Clin Oncol* 2020;38:20–8.
68. Phillips D, Matusiak M, Gutierrez BR, Bhate SS, Barlow GL, Jiang S, et al. Immune cell topography predicts response to PD-1 blockade in cutaneous T cell lymphoma. *Nat Commun* 2021;12:6726.
69. Kim R, An M, Lee H, Mehta A, Heo YJ, Kim K-M, et al. Early tumor-immune microenvironmental remodeling and response to first-line fluoropyrimidine and platinum chemotherapy in advanced gastric cancer. *Cancer Discov* 2022;12:984–1001.
70. Lu G, Baertsch MA, Hickey JW, Goltsev Y, Rech AJ, Mani L, et al. A real-time GPU-accelerated parallelized image processor for large-scale multiplexed fluorescence microscopy data. *Front Immunol* 2022;13:981825.
71. Brbić M, Cao K, Hickey JW, Tan Y, Snyder MP, Nolan GP, et al. Annotation of spatially resolved single-cell data with STELLAR. *Nat Methods* 2022;19:1411–8.
72. Castro LNG, Tirosh I, Suvà ML. Decoding cancer biology one cell at a time. *Cancer Discov* 2021;11:960–70.
73. Lähnemann D, Köster J, Szczurek E, McCarthy DJ, Hicks SC, Robinson MD, et al. Eleven grand challenges in single-cell data science. *Genome Biol* 2020;21:31.
74. De Simone M, Rossetti G, Pagani M. Single cell T cell receptor sequencing: techniques and future challenges. *Front Immunol* 2018;9:1638.
75. Gohil SH, Iorgulescu JB, Braun DA, Keskin DB, Livak KJ. Applying high-dimensional single-cell technologies to the analysis of cancer immunotherapy. *Nat Rev Clin Oncol* 2021;18:244–56.
76. Tirosh I, Venteicher AS, Hebert C, Escalante LE, Patel AP, Yizhak K, et al. Single-cell RNA-seq supports a developmental hierarchy in human oligodendrogloma. *Nature* 2016;539:309–13.
77. La Manno G, Soldatov R, Zeisel A, Braun E, Hochgerner H, Petukhov V, et al. RNA velocity of single cells. *Nature* 2018;560:494–8.
78. Tang F, Barbacioru C, Wang Y, Nordman E, Lee C, Xu N, et al. mRNA-seq whole-transcriptome analysis of a single cell. *Nat Methods* 2009;6:377–82.
79. Islam S, Kjällquist U, Moliner A, Zajac P, Fan J-B, Lönnérberg P, et al. Characterization of the single-cell transcriptional landscape by highly multiplex RNA-seq. *Genome Res* 2011;21:1160–7.
80. Hashimshony T, Wagner F, Sher N, Yanai I. CEL-seq: single-cell RNA-seq by multiplexed linear amplification. *Cell Rep* 2012;2:666–73.
81. Klein AM, Mazutis L, Akartuna I, Tallapragada N, Veres A, Li V, et al. Droplet barcoding for single-cell transcriptomics applied to embryonic stem cells. *Cell* 2015;161:1187–201.
82. Macosko EZ, Basu A, Satija R, Nemesh J, Shekhar K, Goldman M, et al. Highly parallel genome-wide expression profiling of individual cells using nanoliter droplets. *Cell* 2015;161:1202–14.
83. Zheng GX, Terry JM, Belgrader P, Ryvkin P, Bent ZW, Wilson R, et al. Massively parallel digital transcriptional profiling of single cells. *Nat Commun* 2017;8:14049.
84. Gierahn TM, Wadsworth MH II, Hughes TK, Bryson BD, Butler A, Satija R, et al. Seq-well: portable, low-cost RNA sequencing of single cells at high throughput. *Nat Methods* 2017;14:395–8.
85. Guruprasad P, Lee YG, Kim KH, Ruella M. The current landscape of single-cell transcriptomics for cancer immunotherapy. *J Exp Med* 2021;218:e20201574.
86. Andor N, Simonds EF, Czerwinski DK, Chen J, Grimes SM, Wood-Bouwens C, et al. Single-cell RNA-Seq of follicular lymphoma reveals malignant B-cell types and coexpression of T-cell immune checkpoints. *Blood* 2019;133:1119–29.
87. Aoki T, Chong LC, Takata K, Milne K, Hav M, Colombo A, et al. Single-cell transcriptome analysis reveals disease-defining T-cell subsets in the tumor microenvironment of classic Hodgkin lymphoma. *Cancer Discov* 2020;10:406–21.
88. Petti AA, Williams SR, Miller CA, Fiddes IT, Srivatsan SN, Chen DY, et al. A general approach for detecting expressed mutations in AML cells using single cell RNA-sequencing. *Nat Commun* 2019;10:3660.
89. Zavidij O, Haradhvala NJ, Mouhieddine TH, Sklavenitis-Pistofidis R, Cai S, Reidy M, et al. Single-cell RNA sequencing reveals compromised immune microenvironment in precursor stages of multiple myeloma. *Nat Cancer* 2020;1:493–506.
90. Durante MA, Rodriguez DA, Kurtenbach S, Kuznetsov JN, Sanchez MI, Decatur CL, et al. Single-cell analysis reveals new evolutionary complexity in uveal melanoma. *Nat Commun* 2020;11:496.
91. Mathewson ND, Ashenberg O, Tirosh I, Gritsch S, Perez EM, Marx S, et al. Inhibitory CD161 receptor identified in glioma-infiltrating T cells by single-cell analysis. *Cell* 2021;184:1281–98.e26.
92. Wu TD, Madireddi S, de Almeida PE, Banchereau R, Chen Y-JJ, Chitre AS, et al. Peripheral T cell expansion predicts tumour infiltration and clinical response. *Nature* 2020;579:274–8.
93. Zhang Q, He Y, Luo N, Patel SJ, Han Y, Gao R, et al. Landscape and dynamics of single immune cells in hepatocellular carcinoma. *Cell* 2019;179:829–45.e20.
94. Li P-H, Kong X-Y, He Y-Z, Liu Y, Peng X, Li Z-H, et al. Recent developments in application of single-cell RNA sequencing in the tumour immune microenvironment and cancer therapy. *Mil Med Res* 2022;9:52.
95. Deng Q, Han G, Puebla-Osorio N, Ma MCJ, Strati P, Chasen B, et al. Characteristics of anti-CD19 CAR T cell infusion products associated with

- efficacy and toxicity in patients with large B cell lymphomas. *Nat Med* 2020; 26:1878–87.
96. Wang Q, Guldner IH, Golomb SM, Sun L, Harris JA, Lu X, et al. Single-cell profiling guided combinatorial immunotherapy for fast-evolving CDK4/6 inhibitor-resistant HER2-positive breast cancer. *Nat Commun* 2019;10: 3817.
  97. Dar RD, Razooky BS, Singh A, Trimeloni TV, McCollum JM, Cox CD, et al. Transcriptional burst frequency and burst size are equally modulated across the human genome. *Proc Natl Acad Sci U S A* 2012;109:17454–9.
  98. Deng Q, Ramsköld D, Reinius B, Sandberg R. Single-cell RNA-seq reveals dynamic, random monoallelic gene expression in mammalian cells. *Science* 2014;343:193–6.
  99. Patel AP, Tirosh I, Trombetta JJ, Shalek AK, Gillespie SM, Wakimoto H, et al. Single-cell RNA-seq highlights intratumoral heterogeneity in primary glioblastoma. *Science* 2014;344:1396–401.
  100. Massoni-Badosa R, Iacono G, Moutinho C, Kulis M, Palau N, Marchese D, et al. Sampling time-dependent artifacts in single-cell genomics studies. *Genome Biol* 2020;21:112.
  101. van den Brink SC, Sage F, Vértesy Á, Spanjaard B, Peterson-Maduro J, Baron CS, et al. Single-cell sequencing reveals dissociation-induced gene expression in tissue subpopulations. *Nat Methods* 2017;14:935–6.
  102. Slyper M, Porter CBM, Ashenberg O, Waldman J, Drokhlyansky E, Wakiro I, et al. A single-cell and single-nucleus RNA-seq toolbox for fresh and frozen human tumors. *Nat Med* 2020;26:792–802.
  103. Habib N, Avraham-David I, Basu A, Burks T, Shekhar K, Hofree M, et al. Massively parallel single-nucleus RNA-seq with DroNc-seq. *Nat Methods* 2017;14:955–8.
  104. Wu H, Kirita Y, Donnelly EL, Humphreys BD. Advantages of single-nucleus over single-cell RNA sequencing of adult kidney: rare cell types and novel cell states revealed in fibrosis. *J Am Soc Nephrol* 2019;30:23–32.
  105. Tran HTN, Ang KS, Chevrier M, Zhang X, Lee NYS, Goh M, et al. A benchmark of batch-effect correction methods for single-cell RNA sequencing data. *Genome Biol* 2020;21:12.
  106. Camp JG, Platt R, Treutlein B. Mapping human cell phenotypes to genotypes with single-cell genomics. *Science* 2019;365:1401–5.
  107. Kelsey G, Stegle O, Reik W. Single-cell epigenomics: recording the past and predicting the future. *Science* 2017;358:69–75.
  108. Vistain LF, Tay S. Single-cell proteomics. *Trends Biochem Sci* 2021;46:661–72.
  109. Liao J, Lu X, Shao X, Zhu L, Fan X. Uncovering an organ's molecular architecture at single-cell resolution by spatially resolved transcriptomics. *Trends Biotechnol* 2021;39:43–58.
  110. Guillaumet-Adkins A, Rodríguez-Esteban G, Mereu E, Mendez-Lago M, Jaitin DA, Villanueva A, et al. Single-cell transcriptome conservation in cryopreserved cells and tissues. *Genome Biol* 2017;18:45.
  111. Martelotto LG, Baslan T, Kendall J, Geyer FC, Burke KA, Spraggan L, et al. Whole-genome single-cell copy number profiling from formalin-fixed paraffin-embedded samples. *Nat Med* 2017;23:376–85.
  112. Nerurkar SN, Goh D, Cheung CCL, Nga PQY, Lim JCT, Yeong JPS. Transcriptional spatial profiling of cancer tissues in the era of immunotherapy: the potential and promise. *Cancers (Basel)* 2020;12:2572.
  113. Ståhl PL, Salmén F, Vickovic S, Lundmark A, Navarro JF, Magnusson J, et al. Visualization and analysis of gene expression in tissue sections by spatial transcriptomics. *Science* 2016;353:78–82.
  114. Gall JG, Pardue ML. Formation and detection of RNA-DNA hybrid molecules in cytological preparations. *Proc Natl Acad Sci U S A* 1969;63:378–83.
  115. John HA, Birnstiel ML, Jones KW. RNA-DNA hybrids at the cytological level. *Nature* 1969;223:582–7.
  116. Harrison PR, Conkie D, Paul J, Jones K. Localisation of cellular globin messenger RNA by *in situ* hybridisation to complementary DNA. *FEBS Lett* 1973;32:109–12.
  117. Langer-Safer PR, Levine M, Ward DC. Immunological method for mapping genes on Drosophila polytene chromosomes. *Proc Natl Acad Sci U S A* 1982;79: 4381–5.
  118. Rudkin GT, Stollar BD. High resolution detection of DNA-RNA hybrids *in situ* by indirect immunofluorescence. *Nature* 1977;265:472–3.
  119. Tautz D, Pfeifle C. A non-radioactive *in situ* hybridization method for the localization of specific RNAs in Drosophila embryos reveals translational control of the segmentation gene hunchback. *Chromosoma* 1989;98:81–5.
  120. Giani AM, Gallo GR, Gianfranceschi L, Formenti G. Long walk to genomics: history and current approaches to genome sequencing and assembly. *Comput Struct Biotechnol J* 2020;18:9–19.
  121. Gossler A, Joyner AL, Rossant J, Skarnes WC. Mouse embryonic stem cells and reporter constructs to detect developmentally regulated genes. *Science* 1989;244:463–5.
  122. O'Kane CJ, Gehring WJ. Detection *in situ* of genomic regulatory elements in *Drosophila*. *Proc Natl Acad Sci U S A* 1987;84:9123–7.
  123. Moses L, Pachter L. Museum of spatial transcriptomics. *Nat Methods* 2022; 19:534–46.
  124. Femino AM, Fay FS, Fogarty K, Singer RH. Visualization of single RNA transcripts *in situ*. *Science* 1998;280:585–90.
  125. Berglund E, Maaskola J, Schultz N, Friedrich S, Marklund M, Bergenstråhl J, et al. Spatial maps of prostate cancer transcriptomes reveal an unexplored landscape of heterogeneity. *Nat Commun* 2018;9:2419.
  126. Thrane K, Eriksson H, Maaskola J, Hansson J, Lundberg J. Spatially resolved transcriptomics enables dissection of genetic heterogeneity in stage III cutaneous malignant melanoma. *Cancer Res* 2018;78:5970–9.
  127. Moncada R, Barkley D, Wagner F, Chiodini M, Devlin JC, Baron M, et al. Integrating microarray-based spatial transcriptomics and single-cell RNA-seq reveals tissue architecture in pancreatic ductal adenocarcinomas. *Nat Biotechnol* 2020;38:333–42.
  128. Marx V. Method of the year: spatially resolved transcriptomics. *Nat Methods* 2021;18:9–14.
  129. Ji AL, Rubin AJ, Thrane K, Jiang S, Reynolds DL, Meyers RM, et al. Multi-modal analysis of composition and spatial architecture in human squamous cell carcinoma. *Cell* 2020;182:497–514.e22.
  130. Andersson A, Larsson L, Stenbeck L, Salmén F, Ehinger A, Wu SZ, et al. Spatial deconvolution of HER2-positive breast cancer delineates tumor-associated cell type interactions. *Nat Commun* 2021;12:6012.
  131. Dieu-Nosjean M-C, Goc J, Giraldo NA, Sautès-Fridman C, Fridman WH. Tertiary lymphoid structures in cancer and beyond. *Trends Immunol* 2014;35:571–80.
  132. Meylan M, Petitprez F, Becht E, Bougoüin A, Pupier G, Calvez A, et al. Tertiary lymphoid structures generate and propagate anti-tumor antibody-producing plasma cells in renal cell cancer. *Immunity* 2022; 55:527–41.e5.
  133. Dhainaut M, Rose SA, Akturk G, Wróblewska A, Nielsen SR, Park ES, et al. Spatial CRISPR genomics identifies regulators of the tumor microenvironment. *Cell* 2022;185:1223–39.e20.
  134. Biancalani T, Scalia G, Buffoni L, Avasthi R, Lu Z, Sanger A, et al. Deep learning and alignment of spatially resolved single-cell transcriptomes with Tangram. *Nat Methods* 2021;18:1352–62.
  135. Dong R, Yuan G-C. SpatialDWLS: accurate deconvolution of spatial transcriptomic data. *Genome Biol* 2021;22:145.
  136. Dries R, Zhu Q, Dong R, Eng C-HL, Li H, Liu K, et al. Giotto: a toolbox for integrative analysis and visualization of spatial expression data. *Genome Biol* 2021;22:78.
  137. Elosua-Bayes M, Nieto P, Mereu E, Gut I, Heyn H. SPOTlight: seeded NMF regression to deconvolute spatial transcriptomics spots with single-cell transcriptomes. *Nucleic Acids Res* 2021;49:e50.
  138. Kleshchevnikov V, Shmatko A, Dann E, Aivazidis A, King HW, Li T, et al. Cell2location maps fine-grained cell types in spatial transcriptomics. *Nat Biotechnol* 2022;40:661–71.
  139. Eisenstein M. How to make spatial maps of gene activity - down to the cellular level. *Nature* 2022;606:1036–8.
  140. Van TM, Blank CU. A user's perspective on GeoMx™ digital spatial profiling. *Immunooncol Technol* 2019;1:11–8.
  141. Stickels RR, Murray E, Kumar P, Li J, Marshall JL, Di Bella DJ, et al. Highly sensitive spatial transcriptomics at near-cellular resolution with Slide-seqV2. *Nat Biotechnol* 2021;39:313–9.
  142. Merritt CR, Ong GT, Church SE, Barker K, Danaher P, Geiss G, et al. Multiplex digital spatial profiling of proteins and RNA in fixed tissue. *Nat Biotechnol* 2020;38:586–99.
  143. Bergholtz H, Carter JM, Cesano A, Cheang MCU, Church SE, Divakar P, et al. Best practices for spatial profiling for breast cancer research with the GeoMx® digital spatial profiler. *Cancers (Basel)* 2021;13:4456.
  144. Carter JM, Polley M-YC, Leon-Ferre RA, Sinnwell J, Thompson KJ, Wang X, et al. Characteristics and spatially defined immune (micro)landscapes of early-stage PD-L1-positive triple-negative breast cancer. *Clin Cancer Res* 2021;27:5628–37.
  145. Zugazagoitia J, Gupta S, Liu Y, Fuhrman K, Gettinger S, Herbst RS, et al. Biomarkers associated with beneficial PD-1 checkpoint blockade in non-small cell lung cancer (NSCLC) identified using high-plex digital spatial profiling. *Clin Cancer Res* 2020;26:4360–8.

146. Wang N, Wang R, Li X, Song Z, Xia L, Wang J, et al. Tumor microenvironment profiles reveal distinct therapy-oriented proteogenomic characteristics in colorectal cancer. *Front Bioeng Biotechnol* 2021;9:757378.
147. Gupta S, Zugazagoitia J, Martinez-Morilla S, Fuhrman K, Rimm DL. Digital quantitative assessment of PD-L1 using digital spatial profiling. *Lab Invest* 2020;100:1311–7.
148. Toki MI, Merritt CR, Wong PF, Smith JW, Kluger HM, Syrigos KN, et al. High-plex predictive marker discovery for melanoma immunotherapy-treated patients using digital spatial profiling. *Clin Cancer Res* 2019;25:5503–12.
149. Roper N, Velez MJ, Chiappori A, Kim YS, Wei JS, Sindiri S, et al. Notch signaling and efficacy of PD-1/PD-L1 blockade in relapsed small cell lung cancer. *Nat Commun* 2021;12:3880.
150. Herrera FG, Ronet C, Ochoa de Olza M, Barras D, Crespo I, Andreatta M, et al. Low-dose radiotherapy reverses tumor immune desertification and resistance to immunotherapy. *Cancer Discov* 2022;12:108–33.
151. Lu Y, Ng AHC, Chow FE, Everson RG, Helmink BA, Tetzlaff MT, et al. Resolution of tissue signatures of therapy response in patients with recurrent GBM treated with neoadjuvant anti-PD1. *Nat Commun* 2021;12:4031.
152. Zhu S, Ma A-H, Zhu Z, Adib E, Rao T, Li N, et al. Synergistic antitumor activity of pan-PI3K inhibition and immune checkpoint blockade in bladder cancer. *J Immunother Cancer* 2021;9:e002917.
153. Uy GL, Aldoss I, Foster MC, Sayre PH, Wieduwilt MJ, Advani AS, et al. Flotetuzumab as salvage immunotherapy for refractory acute myeloid leukemia. *Blood* 2021;137:751–62.
154. Campbell KM, Thaker M, Medina E, Kalbasi A, Singh A, Ribas A, et al. Spatial profiling reveals association between WNT pathway activation and T-cell exclusion in acquired resistance of synovial sarcoma to NY-ESO-1 transgenic T-cell therapy. *J Immunother Cancer* 2022;10:e004190.
155. Narayan V, Barber-Rotenberg JS, Jung I-Y, Lacey SF, Rech AJ, Davis MM, et al. PSMA-targeting TGFβ-insensitive armored CAR T cells in metastatic castration-resistant prostate cancer: a phase 1 trial. *Nat Med* 2022;28:724–34.
156. Norris JL, Caprioli RM. Analysis of tissue specimens by matrix-assisted laser desorption/ionization imaging mass spectrometry in biological and clinical research. *Chem Rev* 2013;113:2309–42.
157. Schwamborn K, Caprioli RM. Molecular imaging by mass spectrometry—looking beyond classical histology. *Nat Rev Cancer* 2010;10:639–46.
158. Seeley EH, Caprioli RM. 3D imaging by mass spectrometry: a new frontier. *Anal Chem* 2012;84:2105–10.
159. Lopez BGC, Kohale IN, Du Z, Korsunsky I, Abdelmoula WM, Dai Y, et al. Multimodal platform for assessing drug distribution and response in clinical trials. *Neuro Oncol* 2022;24:64–77.
160. Ščupáková K, Adelaja OT, Balluff B, Ayyappan V, Tressler CM, Jenkinson NM, et al. Clinical importance of high-mannose, fucosylated, and complex N-glycans in breast cancer metastasis. *JCI Insight* 2021;6:e146945.
161. Qin L, Zhang Y, Liu Y, He H, Han M, Li Y, et al. Recent advances in matrix-assisted laser desorption/ionisation mass spectrometry imaging (MALDI-MSI) for in situ analysis of endogenous molecules in plants. *Phytochem Anal* 2018;29:351–64.
162. Touboul D, Laprévote O, Brunelle A. Micrometric molecular histology of lipids by mass spectrometry imaging. *Curr Opin Chem Biol* 2011;15:725–32.
163. Briggs D. Recent advances in secondary ion mass spectrometry (SIMS) for polymer surface analysis. *Br Polym J* 1989;21:3–15.
164. Flinders B, Cuypers E, Zeijlemaker H, Tytgat J, Heeren RM. Preparation of longitudinal sections of hair samples for the analysis of cocaine by MALDI-MS/MS and TOF-SIMS imaging. *Drug Test Anal* 2015;7:859–65.
165. Gamble LJ, Anderton CR. Secondary ion mass spectrometry imaging of tissues, cells, and microbial systems. *Microsc Today* 2016;24:24–31.
166. Kaya I, Jennische E, Lange S, Malmberg P. Dual polarity MALDI imaging mass spectrometry on the same pixel points reveals spatial lipid localizations at high-spatial resolutions in rat small intestine. *Anal Methods* 2018;10:2428–35.
167. Passarelli MK, Pirkli A, Moellers R, Grinfeld D, Kollmer F, Havelund R, et al. The 3D OrbiSIMS-label-free metabolic imaging with subcellular lateral resolution and high mass-resolving power. *Nat Methods* 2017;14:1175–83.
168. Tian H, Rabbani SSN, Vickerman JC, Winograd N. Multiomics imaging using high-energy water gas cluster ion beam secondary ion mass spectrometry [(H<sub>2</sub>O)<sub>n</sub>]-GCIB-SIMS] of frozen-hydrated cells and tissue. *Anal Chem* 2021;93:7808–14.
169. Cooks RG, Ouyang Z, Takats Z, Wiseman JM. Detection technologies. Ambient mass spectrometry. *Science* 2006;311:1566–70.
170. Takáts Z, Wiseman JM, Gologan B, Cooks RG. Mass spectrometry sampling under ambient conditions with desorption electrospray ionization. *Science* 2004;306:471–3.
171. Laskin J, Heath BS, Roach PJ, Cazares L, Semmes OJ. Tissue imaging using nanospray desorption electrospray ionization mass spectrometry. *Anal Chem* 2012;84:141–8.
172. Wiseman JM, Ifa DR, Zhu Y, Kissinger CB, Manicke NE, Kissinger PT, et al. Desorption electrospray ionization mass spectrometry: imaging drugs and metabolites in tissues. *Proc Natl Acad Sci U S A* 2008;105:18120–5.
173. Banerjee S. Ambient ionization mass spectrometry imaging for disease diagnosis: excitements and challenges. *J Biosci* 2018;43:731–8.
174. Rocha B, Ruiz-Romero C, Blanco FJ. Mass spectrometry imaging: a novel technology in rheumatology. *Nat Rev Rheumatol* 2017;13:52–63.
175. Saudemont P, Quanico J, Robin Y-M, Baud A, Balog J, Fatou B, et al. Real-time molecular diagnosis of tumors using water-assisted laser desorption/ionization mass spectrometry technology. *Cancer Cell* 2018;34:840–51.e4.
176. Dexter A, Steven RT, Patel A, Dailey LA, Taylor AJ, Ball D, et al. Imaging drugs, metabolites and biomarkers in rodent lung: a DESI MS strategy for the evaluation of drug-induced lipidosis. *Anal Bioanal Chem* 2019;411:8023–32.
177. Santoro AL, Drummond RD, Silva IT, Ferreira SS, Juliano L, Vendramini PH, et al. In situ DESI-MSI lipidomic profiles of breast cancer molecular subtypes and precursor lesions. *Cancer Res* 2020;80:1246–57.
178. Caprioli RM, Farmer TB, Gile J. Molecular imaging of biological samples: localization of peptides and proteins using MALDI-TOF MS. *Anal Chem* 1997;69:4751–60.
179. Liu H, Han M, Li J, Qin L, Chen L, Hao Q, et al. A caffeic acid matrix improves in situ detection and imaging of proteins with high molecular weight close to 200,000 Da in tissues by matrix-assisted laser desorption/ionization mass spectrometry imaging. *Anal Chem* 2021;93:11920–8.
180. He MJ, Pu W, Wang X, Zhang W, Tang D, Dai Y. Comparing DESI-MSI and MALDI-MSI mediated spatial metabolomics and their applications in cancer studies. *Front Oncol* 2022;12:891018.
181. Kompauer M, Heiles S, Spengler B. Atmospheric pressure MALDI mass spectrometry imaging of tissues and cells at 1.4-μm lateral resolution. *Nat Methods* 2017;14:90–6.
182. Prentice BM, Chumbley CW, Caprioli RM. High-speed MALDI MS/MS imaging mass spectrometry using continuous raster sampling. *J Mass Spectrom* 2016;51:665.
183. Galli M, Zoppis I, Smith A, Magni F, Mauri G. Machine learning approaches in MALDI-MSI: clinical applications. *Expert Rev Proteomics* 2016;13:685–96.
184. Jones EE, Gao P, Smith CD, Norris JS, Drake RR. Tissue biomarkers of drug efficacy: case studies using a MALDI-MSI workflow. *Bioanalysis* 2015;7:2611–9.
185. Spencer CE, Flint LE, Duckett CJ, Cole LM, Cross N, Smith DP, et al. Role of MALDI-MSI in combination with 3D tissue models for early stage efficacy and safety testing of drugs and toxicants. *Expert Rev Proteomics* 2020;17:827–41.
186. Harkin C, Smith KW, Cruickshank FL, Logan Mackay C, Flinders B, Heeren RMA, et al. On-tissue chemical derivatization in mass spectrometry imaging. *Mass Spectrom Rev* 2022;41:662–94.
187. Wang X, Han J, Yang J, Pan J, Borchers CH. Matrix coating assisted by an electric field (MCAEF) for enhanced tissue imaging by MALDI-MS. *Chem Sci* 2015;6:729–38.
188. Wang X, Han J, Chou A, Yang J, Pan J, Borchers CH. Hydroxyflavones as a new family of matrices for MALDI tissue imaging. *Anal Chem* 2013;85:7566–73.
189. Wang X, Han J, Pan J, Borchers CH. Comprehensive imaging of porcine adrenal gland lipids by MALDI-FTMS using quercetin as a matrix. *Anal Chem* 2014;86:638–46.
190. Bien T, Perl M, Machmüller AC, Nitsche U, Conrad A, Johannes L, et al. MALDI-2 mass spectrometry and immunohistochemistry imaging of Gb3Cer, Gb4Cer, and further glycosphingolipids in human colorectal cancer tissue. *Anal Chem* 2020;92:7096–105.
191. Niehaus M, Soltwisch J, Belov ME, Dreisewerd K. Transmission-mode MALDI-2 mass spectrometry imaging of cells and tissues at subcellular resolution. *Nat Methods* 2019;16:925–31.
192. Soltwisch J, Kettling H, Vens-Cappell S, Wiegelmann M, Müthing J, Dreisewerd K. Mass spectrometry imaging with laser-induced postionization. *Science* 2015;348:211–5.
193. Brockmann EU, Potthoff A, Tortorella S, Soltwisch J, Dreisewerd K. Infrared MALDI mass spectrometry with laser-induced postionization for imaging of bacterial colonies. *J Am Soc Mass Spectrom* 2021;32:1053–64.

194. Kouzel IU, Soltwisch J, Pohlentz G, Schmitz JS, Karch H, Dreisewerd K, et al. Infrared MALDI mass spectrometry imaging of TLC-separated glycosphingolipids with emphasis on Shiga toxin receptors isolated from human colon epithelial cells. *Int J Mass Spectrom* 2017;416:53–60.
195. Schneemann J, Schäfer K-C, Spengler B, Heiles S. IR-MALDI mass spectrometry imaging with plasma post-ionization of nonpolar metabolites. *Anal Chem* 2022;94:16086–94.
196. Michael JA, Mutuku SM, Ucur B, Sarreto T, Maccarone AT, Niehaus M, et al. Mass spectrometry imaging of lipids using MALDI coupled with plasma-based post-ionization on a trapped ion mobility mass spectrometer. *Anal Chem* 2022;94:17494–503.
197. Spraggins JM, Djambazova KV, Rivera ES, Migas LG, Neumann EK, Fuetterer A, et al. High-performance molecular imaging with MALDI trapped ion-mobility time-of-flight (timsTOF) mass spectrometry. *Anal Chem* 2019;91:14552–60.
198. Sobsey CA, Ibrahim S, Richard VR, Gaspar V, Mitsa G, Lacasse V, et al. Targeted and untargeted proteomics approaches in biomarker development. *Proteomics* 2020;20:e1900029.
199. Fenn JB, Mann M, Meng CK, Wong SF, Whitehouse CM. Electrospray ionization for mass spectrometry of large biomolecules. *Science* 1989;246:64–71.
200. Beck S, Michalski A, Raether O, Lubeck M, Kaspar S, Goedecke N, et al. The impact II, a very high-resolution quadrupole time-of-flight instrument (QTOF) for deep shotgun proteomics. *Mol Cell Proteomics* 2015;14:2014–29.
201. Meier F, Brunner A-D, Frank M, Ha A, Bludau I, Voytik E, et al. diaPASEF: parallel accumulation-serial fragmentation combined with data-independent acquisition. *Nat Methods* 2020;17:1229–36.
202. Volpe P, Eremenko-Volpe T. Quantitative studies on cell proteins in suspension cultures. *Eur J Biochem* 1970;12:195–200.
203. Zhu Y, Piehowski PD, Zhao R, Chen J, Shen Y, Moore RJ, et al. Nanodroplet processing platform for deep and quantitative proteome profiling of 10 to 100 mammalian cells. *Nat Commun* 2018;9:882.
204. Bekker-Jensen DB, Kelstrup CD, Bath TS, Larsen SC, Haldrup C, Bramsen JB, et al. An optimized shotgun strategy for the rapid generation of comprehensive human proteomes. *Cell Syst* 2017;4:587–99.e4.
205. Mund A, Brunner A-D, Mann M. Unbiased spatial proteomics with single-cell resolution in tissues. *Mol Cell* 2022;82:2335–49.
206. Budnik B, Levy E, Harmange G, Slavov N. SCOPE-MS: mass spectrometry of single mammalian cells quantifies proteome heterogeneity during cell differentiation. *Genome Biol* 2018;19:161.
207. Nwosu AJ, Misal SA, Truong T, Carson RH, Webber KGI, Axtell NB, et al. In-depth mass spectrometry-based proteomics of formalin-fixed, paraffin-embedded tissues with a spatial resolution of 50–200 µm. *J Proteome Res* 2022;21:2237–45.
208. Zhu Y, Dou M, Piehowski PD, Liang Y, Wang F, Chu RK, et al. Spatially resolved proteome mapping of laser capture microdissected tissue with automated sample transfer to nanodroplets. *Mol Cell Proteomics* 2018;17:1864–74.
209. Harel M, Ortenberg R, Varanasi SK, Mangalhara KC, Mardamshina M, Markovits E, et al. Proteomics of melanoma response to immunotherapy reveals mitochondrial dependence. *Cell* 2019;179:236–50.e18.
210. Szadai L, Velasquez E, Szeitz B, de Almeida NP, Domont G, Betancourt LH, et al. Deep proteomic analysis on biobanked paraffine-archived melanoma with prognostic/predictive biomarker read-out. *Cancers (Basel)* 2021;13:6105.
211. Berghmans E, Jacobs J, Deben C, Hermans C, Broeckx G, Smits E, et al. Mass spectrometry imaging reveals neutrophil defensins as additional biomarkers for anti-PD-(L)1 immunotherapy response in NSCLC patients. *Cancers (Basel)* 2020;12:863.
212. Beck L, Harel M, Yu S, Markovits E, Boursi B, Markel G, et al. Clinical proteomics of metastatic melanoma reveals profiles of organ specificity and treatment resistance. *Clin Cancer Res* 2021;27:2074–86.
213. Haragan A, Liebler DC, Das DM, Soper MD, Morrison RD, Slebos RJC, et al. Accelerated instability testing reveals quantitative mass spectrometry overcomes specimen storage limitations associated with PD-L1 immunohistochemistry. *Lab Invest* 2020;100:874–86.
214. Liebler DC, Holzer TR, Haragan A, Morrison RD, O'Neill Reising L, Ackermann BL, et al. Analysis of immune checkpoint drug targets and tumor prototypes in non-small cell lung cancer. *Sci Rep* 2020;10:9805.
215. Morales-Betanzos CA, Lee H, Ericsson PIG, Balko JM, Johnson DB, Zimmerman LJ, et al. Quantitative mass spectrometry analysis of PD-L1 protein expression, N-glycosylation and expression stoichiometry with PD-1 and PD-L2 in human melanoma. *Mol Cell Proteomics* 2017;16:1705–17.
216. Whiteaker JR, Lunde RA, Zhao L, Schoenherr RM, Burian A, Huang D, et al. Targeted mass spectrometry enables multiplexed quantification of immunomodulatory proteins in clinical biospecimens. *Front Immunol* 2021;12:765898.
217. Zhang Q, Salzler R, Dore A, Yang J, Ma D, Olson WC, et al. Multiplex immuno-liquid chromatography-mass spectrometry-parallel reaction monitoring (LC-MS-PRM) quantitation of CD8A, CD4, LAG3, PD1, PD-L1, and PD-L2 in frozen human tissues. *J Proteome Res* 2018;17:3932–40.
218. Zhu Y, Zalaznick J, Slezcka B, Parrish K, Yang Z, Olah T, et al. Immunoaffinity microflow liquid chromatography/tandem mass spectrometry for the quantitation of PD1 and PD-L1 in human tumor tissues. *Rapid Commun Mass Spectrom* 2020;34:e8896.
219. Lacasse V, Richard V, Wang H, Mitsa G, Poetz O, Papadakis AI, et al. Immuno-multiple reaction monitoring (iMRM) for quantitation of PD-L1 and PD-1-signaling proteins in non-small cell lung carcinoma (NSCLC). *J Clin Oncol* 2022;40(Suppl 16):2627.
220. Ibrahim S, Lan C, Chabot C, Mitsa G, Buchanan M, Aguilar-Mahecha A, et al. Precise quantitation of pten by immuno-MRM: a tool to resolve the breast cancer biomarker controversy. *Anal Chem* 2021;93:10816–24.
221. Ibrahim S, Froehlich BC, Aguilar-Mahecha A, Aloyz R, Poetz O, Basik M, et al. Using two peptide isotopologues as internal standards for the streamlined quantification of low-abundance proteins by immuno-MRM and immuno-MALDI. *Anal Chem* 2020;92:12407–14.
222. Tobias F, Hummon AB. Considerations for MALDI-based quantitative mass spectrometry imaging studies. *J Proteome Res* 2020;19:3620–30.
223. Agrawal L, Engel KB, Greytak SR, Moore HM. Understanding preanalytical variables and their effects on clinical biomarkers of oncology and immunotherapy. *Semin Cancer Biol* 2018;52:26–38.
224. Gastman B, Agarwal PK, Berger A, Boland G, Broderick S, Butterfield LH, et al. Defining best practices for tissue procurement in immunotherapy clinical trials: consensus statement from the Society for Immunotherapy of Cancer Surgery Committee. *J Immunother Cancer* 2020;8:e001583.
225. Aguilar-Mahecha A, Lafleur J, Pelmas M, Seguin C, Lan C, Discepola F, et al. The identification of challenges in tissue collection for biomarker studies: the Q-CROC-03 neoadjuvant breast cancer translational trial experience. *Mod Pathol* 2017;30:1567–76.
226. Sade-Feldman M, Yizhak K, Bjorgaard SL, Ray JP, de Boer CG, Jenkins RW, et al. Defining T cell states associated with response to checkpoint immunotherapy in melanoma. *Cell* 2018;175:998–1013.e20.
227. Frazao A, Messaoudene M, Nunez N, Dulphy N, Roussin F, Sedlik C, et al. CD16<sup>+</sup>NKG2A<sup>high</sup> natural killer cells infiltrate breast cancer-draining lymph nodes. *Cancer Immunol Res* 2019;7:208–18.
228. Núñez NG, Tosello Boari J, Ramos RN, Richer W, Cagnard N, Anderfuhren CD, et al. Tumor invasion in draining lymph nodes is associated with Treg accumulation in breast cancer patients. *Nat Commun* 2020;11:3272.
229. Chen P-L, Roh W, Reuben A, Cooper ZA, Spencer CN, Prieto PA, et al. Analysis of immune signatures in longitudinal tumor samples yields insight into biomarkers of response and mechanisms of resistance to immune checkpoint blockade. *Cancer Discov* 2016;6:827–37.
230. Basik M, Aguilar-Mahecha A, Rousseau C, Diaz Z, Tejpar S, Spatz A, et al. Biopsies: next-generation biospecimens for tailoring therapy. *Nat Rev Clin Oncol* 2013;10:437–50.
231. Yang SYC, Lien SC, Wang BX, Clouthier DL, Hanna Y, Cirlan I, et al. Pan-cancer analysis of longitudinal metastatic tumors reveals genomic alterations and immune landscape dynamics associated with pembrolizumab sensitivity. *Nat Commun* 2021;12:5137.
232. Annaratone L, De Palma G, Bonizzi G, Sapino A, Botti G, Berrino E, et al. Basic principles of biobanking: from biological samples to precision medicine for patients. *Virchows Arch* 2021;479:233–46.
233. Miao Z, Humphreys BD, McMahon AP, Kim J. Multi-omics integration in the age of million single-cell data. *Nat Rev Nephrol* 2021;17:710–24.
234. Sumida TS, Hafler DA. Population genetics meets single-cell sequencing. *Science* 2022;376:134–5.
235. Kharchenko PV. The triumphs and limitations of computational methods for scRNA-seq. *Nat Methods* 2021;18:723–32.
236. Wang N, Li X, Wang R, Ding Z. Spatial transcriptomics and proteomics technologies for deconvoluting the tumor microenvironment. *Biotechnol J* 2021;16:e2100041.

237. Hickey JW, Tan Y, Nolan GP, Goltsev Y. Strategies for accurate cell type identification in CODEX multiplexed imaging data. *Front Immunol* 2021;12:727626.
238. Mund A, Coscia F, Kriston A, Hollandi R, Kovács F, Brunner AD, et al. Deep visual proteomics defines single-cell identity and heterogeneity. *Nat Biotechnol* 2022;40:1231–40.
239. Akturk G, Sweeney R, Remark R, Merad M, Gnjatic S. Multiplexed immunohistochemical consecutive staining on single slide (MICSSS): multiplexed chromogenic IHC assay for high-dimensional tissue analysis. *Methods Mol Biol* 2020;2055:497–519.
240. Rao A, Barkley D, França GS, Yanai I. Exploring tissue architecture using spatial transcriptomics. *Nature* 2021;596:211–20.
241. Harrell FE. Regression modeling strategies: with applications to linear models, logistic and ordinal regression, and survival analysis. Cham: Springer; 2015.
242. Acharjee A, Kloosterman B, Visser RG, Maliepaard C. Integration of multi-omics data for prediction of phenotypic traits using random forest. *BMC Bioinformatics* 2016;17(Suppl 5):180.
243. Argelaguet R, Velten B, Arnol D, Dietrich S, Zenz T, Marioni JC, et al. Multi-omics factor analysis-a framework for unsupervised integration of multi-omics data sets. *Mol Syst Biol* 2018;14:e8124.
244. Wang T, Shao W, Huang Z, Tang H, Zhang J, Ding Z, et al. MOGONET integrates multi-omics data using graph convolutional networks allowing patient classification and biomarker identification. *Nat Commun* 2021;12:3445.
245. Salmon H, Remark R, Gnjatic S, Merad M. Host tissue determinants of tumour immunity. *Nat Rev Cancer* 2019;19:215–27.